Geology and geochemistry of mafic to felsic plutonic rocks in the Cretaceous intrusive suite of Yosemite Valley, California

Kent Ratajeski*
Allen F. Glazner
Brent V. Miller
Department of Geological Sciences, University of North Carolina, Chapel Hill, North Carolina 27599-3315, USA

ABSTRACT

The intrusive suite of Yosemite Valley provides an excellent example of coeval mafic and felsic magmatism in a continental-margin arc. Within the suite, hornblende gabbros and diorites associated with the Cretaceous El Capitan and Taft Granites occur as scattered mafic enclaves, enclave swarms, small pods, synplutonic dikes, and a 2 km^2 mafic complex known as the ''diorite of the Rockslides.'' Field evidence suggests that most of the mafic rocks are temporally related to the El Capitan Granite and that significantly less mafic magma accompanied the slightly later intrusion of the Taft Granite. Concordant zircon fractions from the diorite of the Rockslides yield an age of 103 ± 0.15 Ma, which is the same age as the El Capitan Granite. Initial isotopic compositions of the mafic and felsic rocks are similar; the mafic rocks exhibit only slightly higher $^{87}Sr/^{86}Sr$, lower $^{143}Nd/^{144}Nd$, and higher $^{206}Pb/^{204}Pb$ ratios than the granites. Because the mafic magmas are only slightly more isotopically evolved than the granites, geochemical variation within the granites is not easily explained in terms of contamination of a depleted-mantle component by partial melts of ancient, high-silica continental crust. Rather, these data are consistent with an interpretation that the El Capitan Granite was derived by partial melting of relatively young mafic sources broadly similar to the mafic rocks of the suite.

Keywords: granite, isotopes, mafic magmas, Sierra Nevada batholith, Yosemite National Park.

*Present address: Department of Geology, Northern Arizona University, Box 4099, Flagstaff, Arizona 86011, USA; e-mail: kent.ratajeski@nau.edu.

INTRODUCTION

The importance of mafic magmatism for the generation of calc-alkalic plutons and batholiths in convergent-margin settings is widely acknowledged. Mafic magmas that are underplated beneath or injected into the lower crust have been called upon as thermal triggers for lower-crustal partial melting (e.g., Hildreth, 1981; Bergantz, 1989), parental magmas for crystallization differentiation (e.g., Bowen, 1928, Bateman and Chappell, 1979), and end-member components of magma mixing (e.g., Allègre and Othman, 1980; Castro et al., 1991).

Historically, large-scale mafic magmatism in ancient arc settings has been inferred largely from geochemical and isotopic studies of the granites (sensu lato) that dominate the upper-crustal parts of arcs. Because of the relative rarity of mafic plutons in granitic batholiths, and perhaps also because of the entrenched notion that mafic plutons are ''precursors'' to the granites, only a few studies of the Sierra Nevada, for example, have examined the relationships between larger exposures of mafic rocks and the nearby granites (Frost and Mahood, 1987; Bradford, 1995; Coleman et al., 1995; Sisson et al., 1996). Much more common are studies of smaller-scale mafic enclaves—quenched volumes of basaltic to dioritic magma entrained within silicic magma chambers (e.g., Furman and Spera, 1985; Barbarin, 1990; Dorais et al., 1990; Didier and Barbarin, 1991). Geochronologic studies of mafic plutons also lag behind those of the more voluminous granites. Relating map-scale exposures of mafic rocks within batholiths to crustal-scale arc petrogenesis remains an important goal in igneous petrology. In this paper we present new field, geochronologic, geochemical, and isotopic data bearing on the relationship of the granitic rocks in western Yosemite Valley to nearby mafic plutonic rocks.

GEOLOGIC SETTING

Yosemite Valley is located in the west-central part of the Sierra Nevada batholith, California. The geology of the western half of the valley (Fig. 1) is dominated by middle Cretaceous (ca. 100 Ma; Stern et al., 1981) granitic rocks associated with the intrusive suite of Yosemite Valley (Bateman, 1992). In the vicinity of Yosemite National Park, plutonic rocks of this suite intrude Paleozoic metasedimentary rocks and granodioritic and tonalitic plutons of the Fine Gold Intrusive Suite (ca. 115 Ma; Bateman, 1992). In the eastern half of Yosemite Valley, granites of the intrusive suite of Yosemite Valley are intruded by Late Cretaceous granodiorites and granites related to the Tuolumne Intrusive Suite (Bateman, 1992), which were emplaced from 95 to 85 Ma (Fleck et al., 1996; Coleman and Glazner, 1997). Intrusive relationships (Calkins et al., 1985) and geochronologic data (Stern et al., 1981) indicate an eastward shift in the locus of magmatism through the Yosemite region during the Cretaceous, a pattern that is reflected in the Cretaceous batholith as a whole (Bateman, 1992).

ROCK UNITS AND FIELD RELATIONSHIPS

Rock units that are currently assigned to the intrusive suite of Yosemite Valley are the El Capitan and Taft Granites (Bateman, 1992). The El Capitan Granite is the older and more voluminous unit of the two and tends to surround smaller masses of Taft Granite. Our

GSA Bulletin; November 2001; v. 113; no. 11; p. 1486–1502; 14 figures; 2 tables; Data Repository item 2001125.

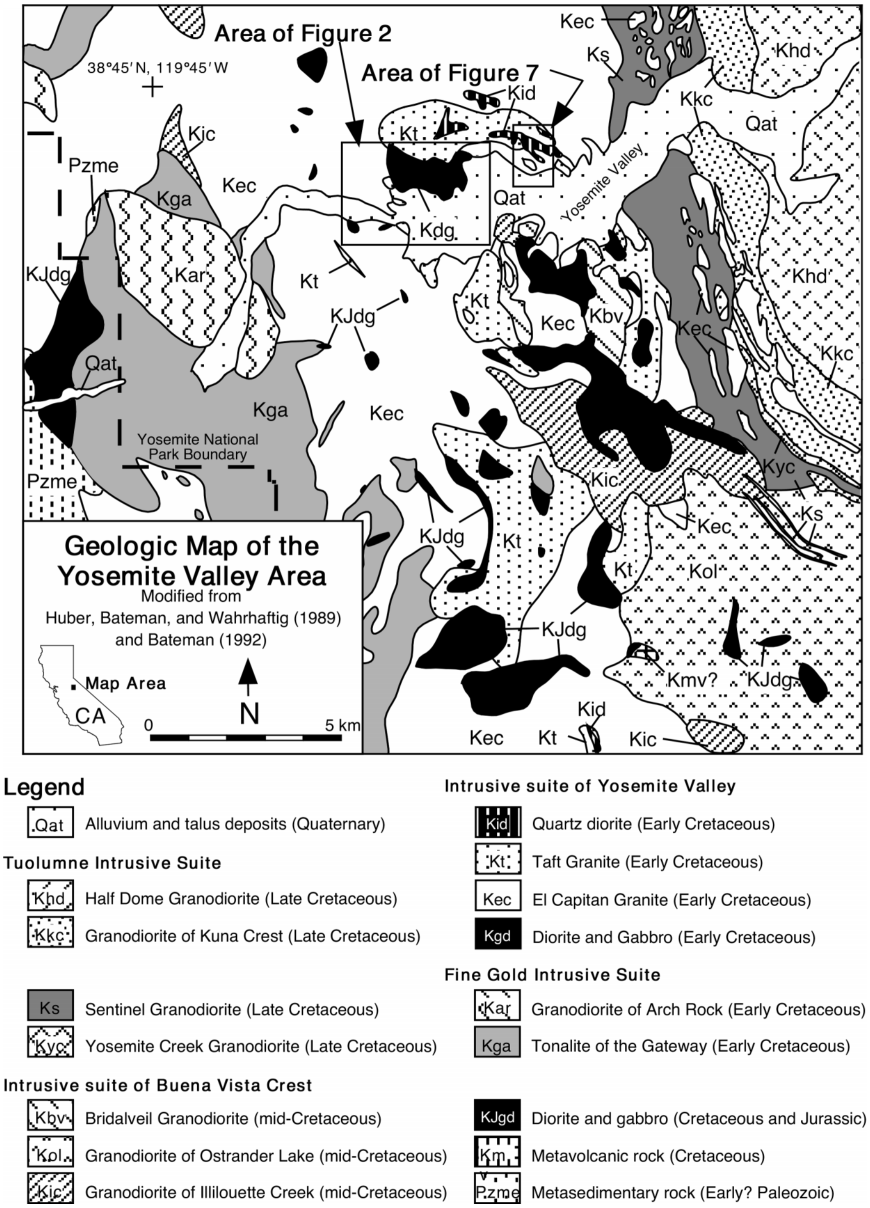

Figure 1. Geology of the western part of Yosemite National Park, modified from Huber, Bateman, and Wahrhaftig (Huber et al., 1989). Diorite and gabbro are abundant in the region and are colored black on the map, regardless of age.

field work suggests that mafic enclaves, schlieren, small pods of mafic rocks, and the diorite of the Rockslides mafic complex are spatially and temporally associated with the El Capitan Granite, whereas the Taft Granite is similarly associated with mafic enclaves, schlieren, and the large mafic dike complex that is visible on the North America Wall of El Capitan (Reid et al., 1983). A steeply dipping, north-northwest–striking foliation is present in many of these rocks; we interpret all foliation described herein to be magmatic. Mafic rocks continue to be spatially associated with these granites for ~10 km to the south, but we have focused almost exclusively on the Yosemite Valley, where a variety of mafic to felsic rock units associated with the intrusive suite of Yosemite Valley are exposed nearly continuously over a 1.2 km vertical section.

Granites

The El Capitan Granite, the dominant geologic unit within the western half of Yosemite Valley (Fig. 2), ranges from coarse-grained biotite granodiorite to biotite granite and is equigranular to porphyritic with potassium feldspar megacrysts (Bateman, 1992). Although the granite shows some limited variability in composition and texture, these features do not appear to describe a regular pattern as for zoned plutons. Concordant U-Pb zircon data suggest an age of 102–103 Ma for the unit (Stern et al., 1981). We attempted to date the El Capitan Granite for this study (see below), but our attempts resulted in discordant data, which plotted slightly below concordia in the vicinity of 102–105 Ma, possibly indicating a combination of Pb loss and inheritance of slightly older zircons.

The Taft Granite (Calkins, 1930) has a lower color index than the El Capitan Granite and a finer-grained, equigranular texture. Most of the Taft Granite is medium grained, but some outcrops are as coarse grained as the equigranular part of the El Capitan Granite. Throughout the western half of Yosemite Valley, Taft Granite forms dikes and larger masses that sharply cut the El Capitan Granite and associated mafic rocks. The precise age of the Taft Granite is unknown. A discordant date of 95 Ma was reported by Stern et al. (1981), and our attempts to date the Taft resulted in discordant data similar to those obtained for the El Capitan Granite.

Granite-Hosted Mafic Enclaves, Schlieren, and Pods

Mafic rocks are locally plentiful in the El Capitan pluton. Enclaves are typically ellipsoidal, dioritic, medium grained, and equigranular to porphyritic; they occur as small (~0.1 m), isolated bodies and in large swarms (Fig. 3A). Some have chilled margins. Those in the larger swarms are usually surrounded by a foliated, granitic matrix, which is depleted in potassium relative to normal El Capitan granite. Porphyritic enclaves contain plagioclase and quartz xenocrysts from the El Capitan Granite (Barbarin, 1990). Plagioclase xenocrysts in porphyritic enclaves are essentially unzoned and have compositions (An_{35-40}) similar to those of the unzoned plagioclase grains in the surrounding granitic matrix and to calcic cores within the El Capitan Granite (Table DR6 in GSA Data Repository[1]). Mafic enclaves, which are less common within the Taft Granite than in the El Capitan Granite, are commonly sheared and grade into schlieren.

A complete gradation in size exists from

[1]GSA Data Repository item 2001125 is available on the Web at http://www.geosociety.org/pubs/ft2001.htm. Requests may also be sent to editing@geosociety.org.

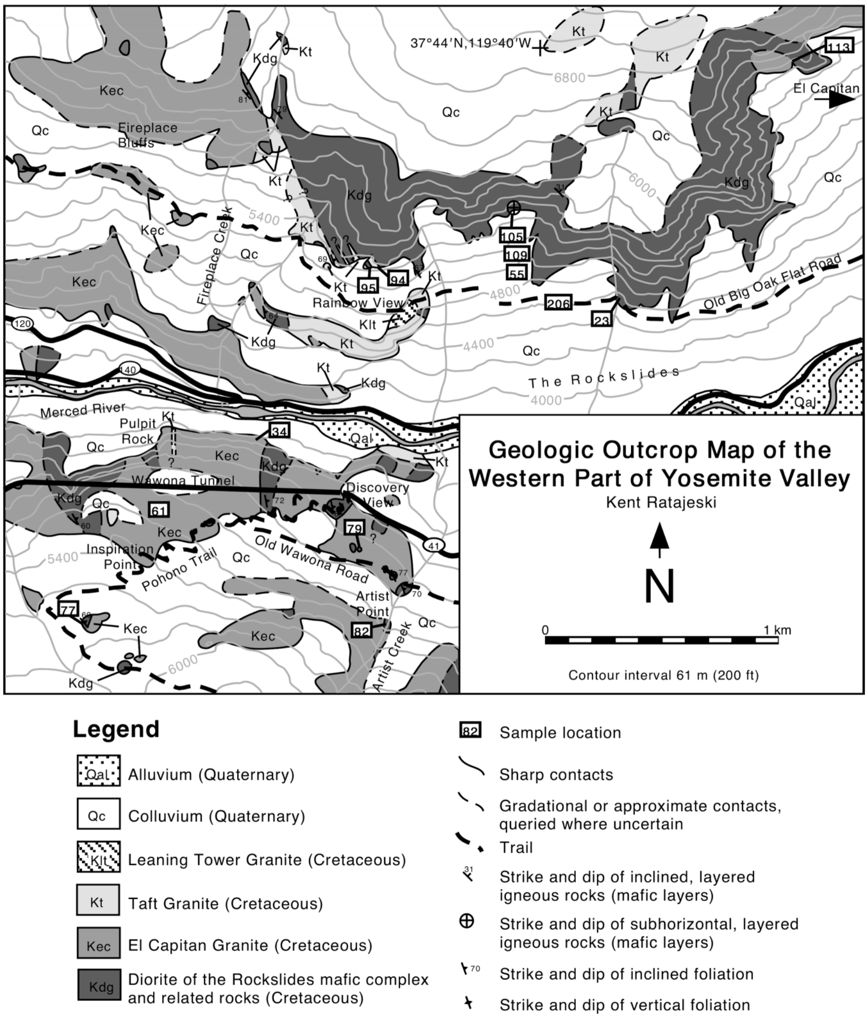

Figure 2. Geologic map of the western part of Yosemite Valley.

decimeter-scale gabbroic to dioritic enclaves hosted by the El Capitan Granite to mappable pods of gabbro and diorite. Mafic pods are concentrated in the El Capitan Granite west of the Rockslides cliffs and across the Merced River near the Pohono Trail (Fig. 2). Pods of mafic rocks associated with the El Capitan Granite are typically composed of medium-grained, equigranular to porphyritic (probably xenocrystic; see below) gabbros and diorites similar to those in mafic enclaves. Pods range in size from small bodies a few meters across (Fig. 3B) to larger bodies hundreds of meters across. Many of these pods are elongated parallel to the regional magmatic foliation. Some diorite pods have relatively sharp contacts against El Capitan Granite; foliation within the diorite generally parallels these contacts. Fine-grained, quenched margins at these contacts are locally present.

Mafic pods are porphyritic only in smaller pods and in the marginal regions of larger pods (Fig. 3C), although it is possible that less noticeable, smaller xenocrysts are present within otherwise equigranular varieties. Obvious xenocrysts in these rocks include rounded quartz with hornblende reaction rims, and plagioclase with core compositions that match calcic plagioclase cores within the El Capitan Granite ($An_{\sim 40}$) (Table DR6 in Data Repository; see text footnote 1). Cores of xenocrystic plagioclase are successively mantled by a highly calcic zone ($An_{\sim 84}$), which probably formed during magma mixing, and then by a rim of An_{40} plagioclase. Groundmass plagioclase in these rocks contains $An_{\sim 79}$ cores and $An_{\sim 41}$ rims. The interiors of plagioclase xenocrysts contain tiny hornblende inclusions (Fig. 4), the origin of which is uncertain, as hornblende is exceedingly rare in the granite. One possibility is that hornblende was a liquidus phase in the granite, but reacted to form biotite during cooling. However, the fact that the hornblende inclusions are identical in composition to hornblende in the groundmass of the mafic rocks suggests that these inclusions may have formed in channel-like cavities within partially resorbed plagioclase during the introduction of the xenocrysts into the mafic magma (R. Wiebe, 1999, personal communication).

Also present within some diorite pods are irregular, foliated ‘‘stringers’’ of leucocratic biotite tonalite or quartz diorite, which commonly separate finger-like splays of hornblende diorite (Fig. 3B). Some stringers can be traced into marginal regions of foliated, leucocratic tonalite to quartz diorite that surround mafic pods within El Capitan Granite (Fig. 3B). These ‘‘marginal sheaths’’ are a few meters thick, and many have sharp contacts against the surrounding, coarser-grained granite. The K-depleted stringers and sheaths probably represent El Capitan Granite that interacted with the mafic magma in the liquid and solid states.

Diorite of the Rockslides Mafic Complex

The diorite of the Rockslides mafic complex (Calkins, 1930; Calkins et al., 1985) occurs in cliff-forming outcrops on the north side of the valley west of El Capitan (Fig. 5A). The extensive talus deposits after which the unit is named are almost entirely composed of boulders derived from this unit; they offer fresher samples and more clearly exposed contact relationships than do the weathered outcrops above. An examination of the talus and outcrops indicates that the diorite constitutes a composite mafic intrusion composed of a variety of different rock types. The term ‘‘diorite of the Rockslides’’ does not refer to a restricted rock type, but to the mafic complex as a whole (Calkins, 1930).

Much of the lithologic diversity within the diorite of the Rockslides mafic complex occupies a broad spectrum between two end-member rock types: (1) a fine- to medium-grained, weakly porphyritic, biotite hornblende gabbro or diorite and (2) a coarser-grained, more leucocratic, equigranular, hornblende biotite quartz diorite or tonalite. Both types are largely free of pyroxene, as clinopyroxene occurs only rarely as small relict cores within hornblende. The finer-grained, more melanocratic gabbro generally occurs as mafic enclaves of various sizes within the leucocratic rock. These mafic enclaves range from randomly oriented, centimeter-scale bodies to meter-thick, pillowed layers similar to those described in other layered mafic-felsic complexes in the Sierra (Bradford, 1995; Coleman et al., 1995; Sisson et al., 1996) and

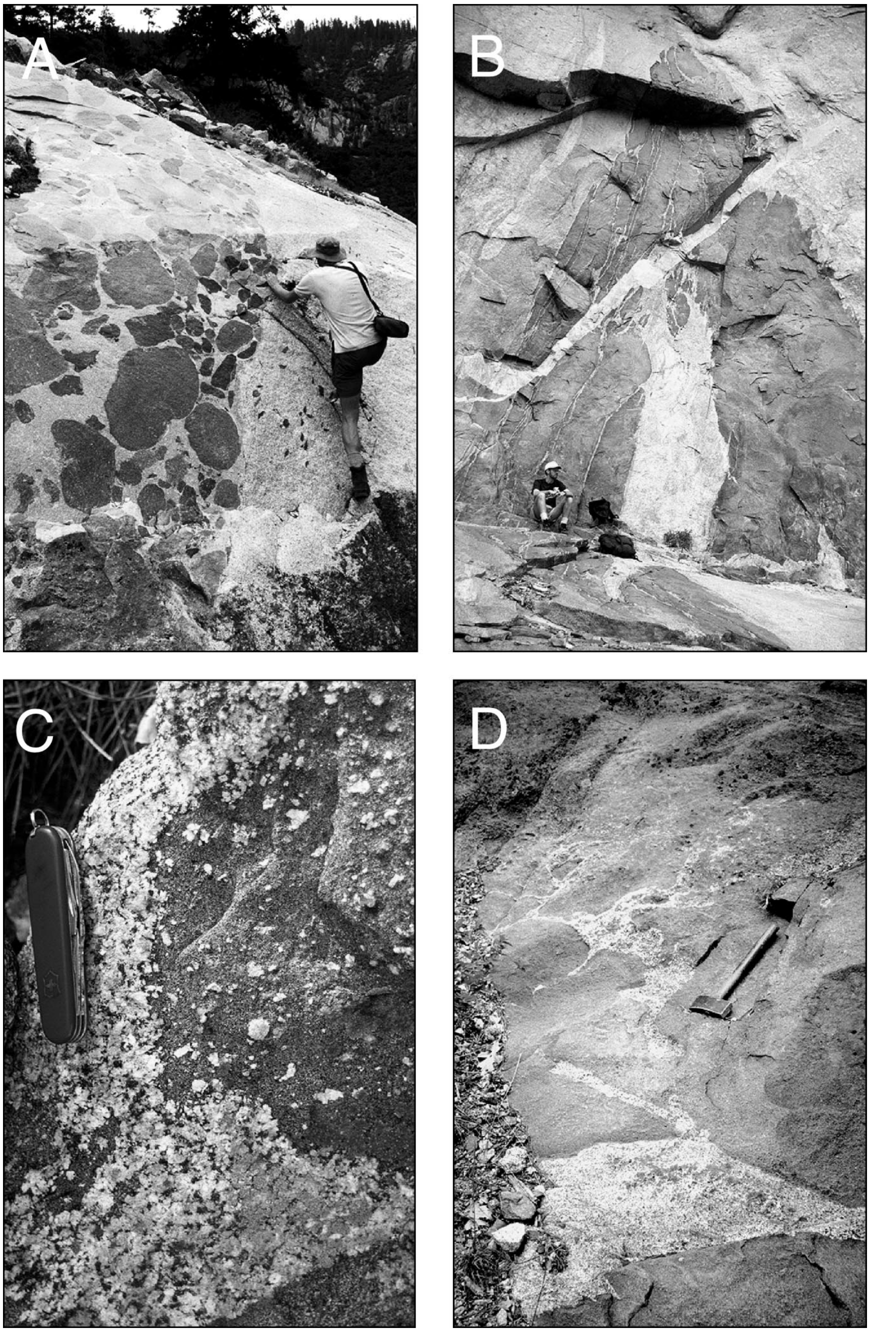

Figure 3. Smaller-scale occurrences of mafic rocks associated with granites of the intrusive suite of Yosemite Valley. (A) Large mafic enclave swarm in El Capitan Granite beside California State Highway 140 near Elephant Rock. (B) Wedge-shaped pod of diorite within El Capitan Granite at the base of the North America Wall of El Capitan. Note the ''stringers'' of foliated leucocratic rock, which trend from upper right to lower left within the left part of the pod. These stringers can be traced into a 0.5–1.5-m-thick ''sheath'' of foliated leucocratic rock, which surrounds the pod. (C) Porphyritic diorite associated with the El Capitan Granite. Feldspar xenocrysts within the diorite were probably derived from the adjacent, partially molten granite. (D) Leucocratic quartz diorite ''stringer'' within pod of diorite near Artist Creek.

elsewhere (e.g., Wiebe, 1993, 1996). In loose boulders and in outcrop (Fig. 5, B and C), meter-thick mafic layers are commonly stacked on top of each other, separated by intervening, 10–25-cm-thick septa of leucocratic, medium-grained tonalite. Outcrops and paleohorizontal indicators within loose blocks of talus (e.g., density-driven structures such as tonalite protrusions into the bottoms of mafic layers; Fig. 5D) indicate an initially subhorizontal orientation of the gabbroic pillows and sheets within the complex. Fresh surfaces on talus reveal quenched, fine-grained margins of the gabbroic layers against the leucocratic tonalite septa. In addition to the rock types already described, rarer orbicular, rhythmically layered, and pegmatitic varieties of mafic rocks also occur within the diorite of the Rockslides mafic complex.

Contacts between that diorite and the El Capitan Granite are exposed in cliffs 0.75 km west of Ribbon Falls and outcrops 0.5 km northeast of Fireplace Bluffs. Near Ribbon Falls, gabbro has chilled against foliated, leucocratic quartz diorite, which in turn grades into weakly foliated, coarse-grained El Capitan Granite. In the exposures near Fireplace Bluffs, diorite is complexly intermingled with El Capitan Granite within a diffuse zone about 0.5 m wide. Porphyritic textures are present in the diorite within this zone but not outside it, suggesting that the feldspar ''phenocrysts'' originated as xenocrysts from the adjacent granite. Field relationships at these two locations, as well as the lack of cutting of the El Capitan Granite by dikes related to the diorite of the Rockslides mafic complex, are consistent with the hypothesis that the diorite was emplaced during the crystallization interval of the El Capitan Granite.

Mafic Dikes Exposed on El Capitan

A sizable mafic dike complex is exposed on the 900-m-high eastern wall (the ''North America Wall'') and summit dome of El Capitan (Fig. 6A). Reid et al. (1983) grouped dikes within this large complex into two sets. The older set, which includes large xenolithic blocks of partially digested El Capitan Granite, is generally moderately dipping, lighter colored, biotite bearing and hornblende poor, and dioritic to granodioritic in composition. The younger set is steeply dipping, generally more mafic and hornblende rich but compositionally diverse, and rich in enclaves. It is composed of two large dikes: a western one shaped like the outline of North America (Fig. 6A) and an eastern one surrounding a large circular area of white El Capitan Granite,

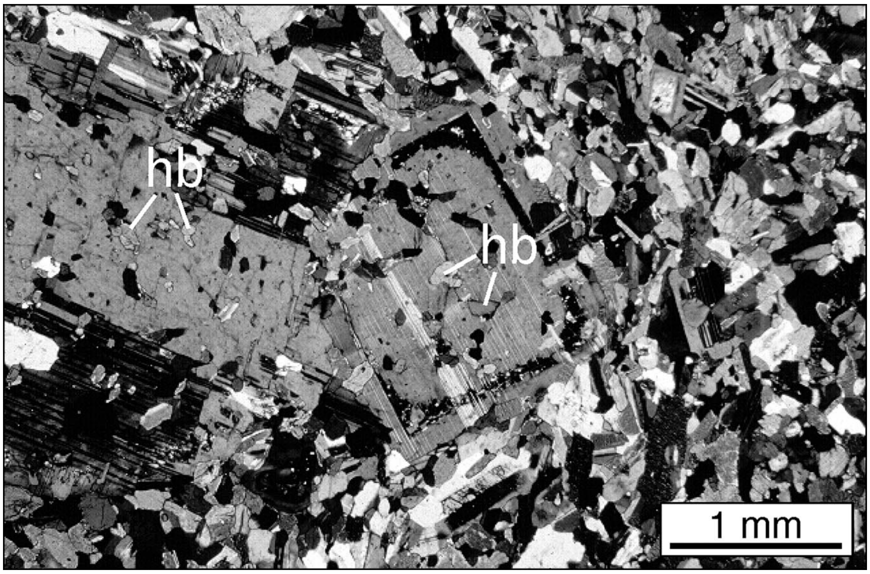

Figure 4. Photomicrograph of a porphyritic (xenocrystic) diorite (sample YOS-77) from a small mafic pod (crossed polarizers). Groundmass consists mostly of plagioclase, hornblende, biotite, and minor quartz. Plagioclase xenocrysts contain partially resorbed cores, calcic zones, and inclusions of hornblende (hb; biotite is absent).

known to rock climbers as the ''Great Circle,'' which is separated from ''North America'' by an intervening ''Atlantic Ocean'' of El Capitan Granite. Following Reid et al. (1983), we refer to both of these large, steeply dipping dikes as North America dikes, and we denote dikes of the older, moderately dipping set as pre–North America dikes.

Our observations at the base of the North America Wall largely confirm the interpretations of Reid et al. (1983) with regard to the field relationships of the mafic dikes and the El Capitan Granite. Pre–North America dikes exposed at the base of this wall have clearly intruded totally solidified El Capitan Granite, locally breaking off and partially assimilating blocks of granite in the process (Fig. 6B). Some of these dikes have sharp contacts against the El Capitan Granite and contain partially mingled mafic and felsic magmas (Fig. 6C).

The younger, North America Wall mafic dikes extend across the summit dome of El Capitan as a series of enclave-choked dikes that strike N60°W (Fig. 7). Contacts with the El Capitan Granite are locally sharp (Fig. 6D), but elsewhere are more gradational, indicating that some interaction—perhaps partial melting and assimilation—with El Capitan Granite has occurred here as well as on the North America Wall. Contacts of the mafic dikes with the Taft Granite are diffuse and characterized by broad zones in which dikes grade into highly elongate schlieren within the Taft Granite (Fig. 6E). Mafic schlieren are also present in narrow dikes of the Taft Granite that cut the El Capitan Granite along the El Capitan Trail 0.5 km north of the summit. In some places on the summit dome, the ''dikes'' are actually planar swarms of mafic enclaves (Tobisch et al., 1997) suspended in a matrix of Taft Granite or remobilized El Capitan Granite. Enclaves in these outcrops are compositionally and texturally diverse and record a complex history of interaction between mafic and felsic magmas (Fig. 6F). The synplutonic character of the North America dikes can be reasonably inferred from these field relationships.

Calkins et al. (1985) mapped a North America mafic dike along the contact of the El Capitan and Taft Granites approximately midway between El Capitan summit and the edge of the North America Wall. Our mapping indicates that a foliated, leucocratic biotite tonalite crops out at this location. This unit displays sharp, interdigitated contacts against the El Capitan Granite, but grades into the adjacent Taft Granite. This tonalite is compositionally very similar to the biotite-rich, hornblende-poor pre–North America mafic dikes that have partially digested quantities of adjacent El Capitan Granite, and it may have formed in a similar manner. Because this unit grades into the Taft Granite and is lithologically similar to it, however, we interpret this unit as representing coeval mafic material (similar to that within the pre–North America dikes) that was mixed within the marginal part of the Taft Granite magma chamber at this location.

These field relationships suggest that the North America mafic dike complex is coeval with the Taft Granite and does not postdate it as previous workers have suggested (Calkins, 1930; Calkins et al., 1985; Bateman, 1992). This interpretation best explains the striking spatial association of the two units on the north side of the valley, where North America mafic dikes are commonly in contact with Taft Granite and generally follow its arcuate map pattern.

GEOCHRONOLOGY

Rationale

As a test of the field interpretations, five samples were selected for conventional U-Pb zircon dating: El Capitan Granite (YOS-180); coarse-grained Taft Granite (YOS-1); a melanocratic, fine- to medium-grained sample of gabbro from the diorite of the Rockslides mafic complex (YOS-23c); a leucocratic, medium- to coarse-grained diorite collected from talus below the cliffs bearing the diorite of the Rockslides mafic complex (YOS-206); and a fine-grained gabbro from the younger set of North America mafic dikes on El Capitan (YOS-104). The methods employed in our analyses are summarized in Appendix 1, and sample locations are tabulated in Table DR1 in Data Repository (see text footnote 1).

U-Pb ages for two fractions of El Capitan Granite zircons have been reported by Stern et al. (1981): one is concordant at 103 Ma, and the other is slightly discordant at ca. 97 Ma. Only one markedly discordant fraction of the Taft Granite (ca. 96 Ma) was analyzed by Stern et al. Since this early work, improvements in the conventional U-Pb zircon technique allow more precise ages to be obtained from smaller, handpicked fractions. No previous geochronologic analyses have been carried out on the mafic rocks.

Results

Isotopic ratios and calculated ages are tabulated in Table 1 and are plotted on a conventional concordia diagram (Fig. 8). Most of the $^{206}Pb/^{238}U$ and $^{207}Pb/^{235}U$ ages fall between 101 and 105 Ma. The $^{207}Pb/^{206}Pb$ ages are considerably older, ranging from 110 to 140 Ma, but there are no linear trends within individual samples for constructing meaningful discordia. Three fractions from the diorite of the Rockslides mafic complex sample YOS-206 are concordant within error at 103.5 $\pm$ 0.15 Ma

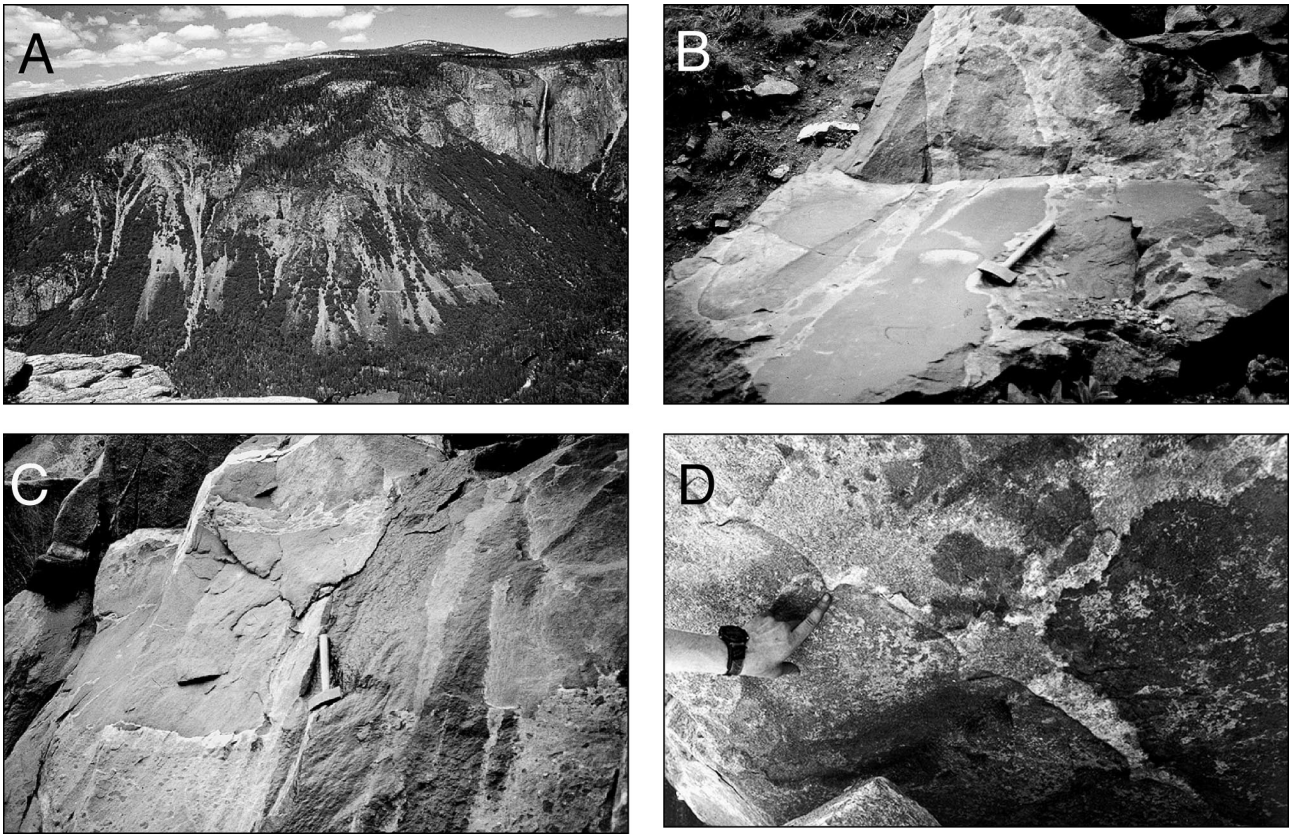

Figure 5. The diorite of the Rockslides mafic complex. (A) Outcrops and talus slopes in the Rockslides area. The El Capitan Granite forms the steep cliffs adjacent to Ribbon Falls in the upper right, and the Taft Granite forms the gently sloping, mostly tree-covered terrain immediately above the Rockslides cliffs (center). (B) Talus boulder in the Rockslides, displaying gabbroic pillows within leucocratic tonalite to quartz diorite host. (C) Subhorizontal gabbroic layers in outcrop, separated by thin, intervening leucocratic septa. The bottommost layer contains dispersed mafic enclaves. Dark, vertical streaks are water. (D) Regularly spaced protrusions of leucocratic tonalite to quartz diorite into mafic pillow within a boulder of talus. Paleo-up is down and to the left.

(MSWD = 0.45, probability of concordance = 0.83; method of Ludwig, 1998). Four additional fractions from this rock form a sublinear array to the right of concordia that yields no meaningful regression. Two of these discordant fractions were analyzed at another geochronology laboratory in order to ensure that discordance is not an analytical artifact (see footnote to Table 1). We, therefore, interpret the concordant fractions to date the crystallization of the diorite of the Rockslides mafic complex and the four other fractions to show variable effects of Pb loss and zircon inheritance from a slightly older source. Our date for the diorite of the Rockslides mafic complex is identical to the 103 Ma date obtained by Stern et al. (1981). Our analyses from another sample of the diorite of the Rockslides mafic complex (YOS-23c), the North America diorite, the El Capitan Granite, and the Taft Granite plot just to the right of concordia at 102–105 Ma (Fig. 8). With larger errors, it would be impossible to tell the difference between this complex discordance and concordant analyses. The pattern of discordance from all five samples suggests that inheritance of ancient (Paleozoic or older) zircons is not a major influence on the U-Pb systematics, but instead that Pb loss and inheritance of only slightly older (Cretaceous or Jurassic?) zircons is a common feature of Sierra Nevadan plutonic rocks. Although the four samples with only discordant analyses provide no precise age information, their true ages are likely to be in the range of 102–105 Ma, which is roughly the range for rocks related to the intrusive suite of Yosemite Valley (Stern et al., 1981). Careful grain selection and high-precision single-grain analyses will be required to better define the ages of the other plutonic units.

GEOCHEMISTRY

Rationale

In order to document the whole-rock compositions of the major rock types that comprise the intrusive suite of Yosemite Valley and to develop petrogenetic hypotheses, 39 fresh samples were analyzed for major element, trace element, and isotopic compositions. Methods employed for the analyses are described in Appendix 2, and the complete data set is available (Tables DR2, DR3, and DR4; see text footnote 1).

Major and Trace Elements

Sampled plutonic rocks associated with the intrusive suite of Yosemite Valley range from 49 to 76 wt% SiO_2 (representative data in Table 2). On SiO_2 variation diagrams, trends in most major elements across the suite are clearly nonlinear (Fig. 9). For Al, Na, and K, in particular, breaks in slope occur at ~65–70 wt% SiO_2, the approximate lower limit of the El Capitan and Taft Granites. Linear trends within the data are limited to the granites and to the mafic dikes exposed on El Capitan. Considerable scatter characterizes mafic samples collected from the diorite of the Rock-

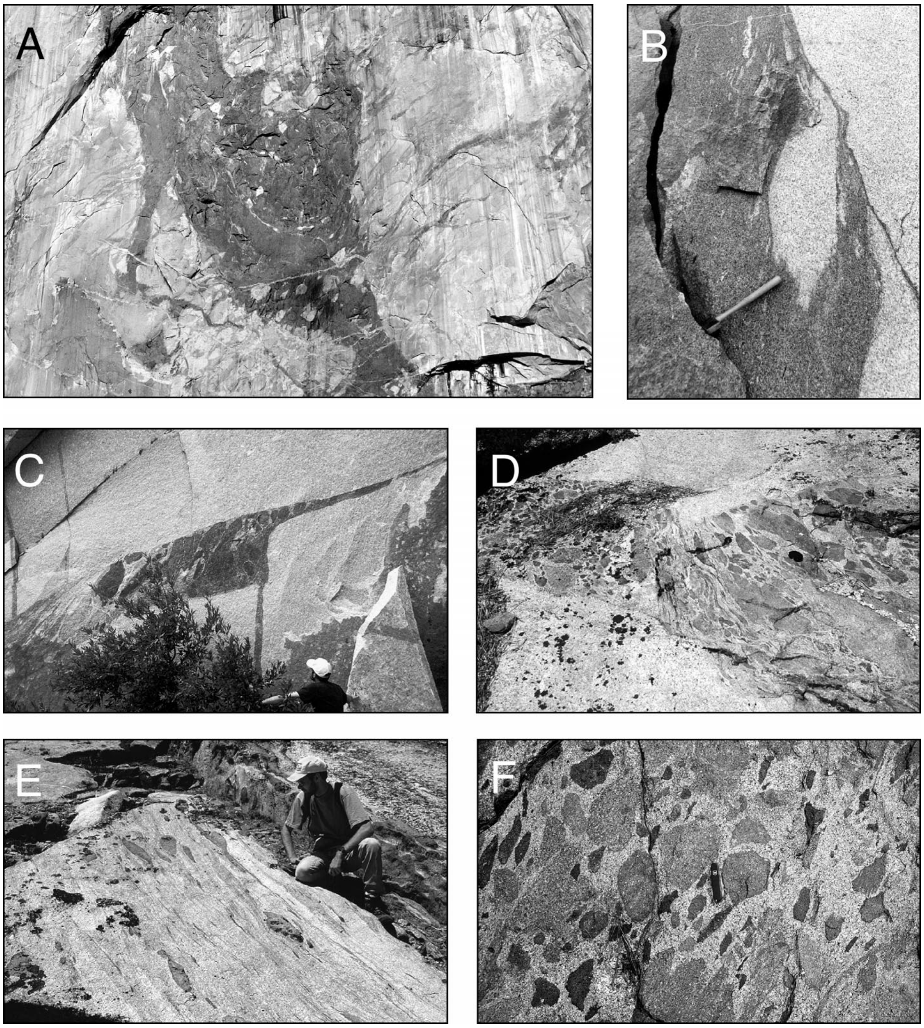

Figure 6. Mafic dikes exposed on El Capitan. (A) Mafic dikes exposed on the North America Wall. Older (pre–North America) dikes within the El Capitan Granite, which trend from lower left to upper right, are cut by the larger, darker-colored dike complex shaped like North America (Reid et al., 1983). The vertical distance in this view is ~450 m. (B) Fairly homogeneous pre–North America mafic dike, frozen in the process of assimilating wall rocks of El Capitan Granite. Unlike other mafic dikes on El Capitan, this dike contains biotite but lacks hornblende. (C) Mingled mafic and felsic magmas in pre–North America mafic dike sharply cutting the El Capitan Granite at the base of the North America Wall. (D) Enclave-choked North America mafic dike in El Capitan Granite on the summit dome of El Capitan. A camera lens cap (~5 cm wide) is placed for scale at the center right. (E) Sheared enclaves and schlieren in diffuse contact zone between Taft Granite and mafic dike photographed in D. (F) Diverse group of mafic enclaves within granitic matrix in synplutonic dike on El Capitan.

slides mafic complex and smaller pods, a feature observed in other mafic complexes in the Sierra Nevada (Sisson et al., 1996).

Not surprisingly, Cr and Ni contents of the mafic rocks (Fig. 10; representative data by DCP-AES [direct current plasma–atomic emission spectrometry] in Table 2) are low compared to values appropriate for primitive arc basalts. Sr contents for noncumulate mafic rocks are in the 400–600 ppm range and do not reach the high values (~650–800 ppm) attained by hornblende gabbros in the Goodale Canyon and Onion Valley mafic complexes in the eastern Sierra Nevada (Bradford, 1995; Sisson et al., 1996), suggesting that the Yosemite mafic rocks are more geochemically removed from their mantle source(s). Elevated contents of Ba, Sr, and LREEs (light rare earth elements) characterize the interlayer septa in the diorite of the Rockslides mafic complex and the marginal sheaths associated with the contacts of mafic pods against granite. Among the granites, Taft Granite sample YOS-210 is notable for its low concentrations of Ba, Sr, and the REEs compared to the other granitic samples.

Radiogenic Isotope Ratios

Initial Sr and Nd isotope ratios (corrected for radiogenic growth since 103 Ma) for all rock types are similar (Fig. 11; representative data in Table 2). Most of the data cluster tightly; $(^{87}Sr/^{86}Sr)_i$ ratios range from 0.7065 to 0.7072, and $\epsilon_{Nd}(t)$ values range from −4 to −6. Compared to the other Sierran intrusive suites plotted in Figure 11, only the Mount Whitney and Tuolumne intrusive suites have lower $\epsilon_{Nd}(t)$ values, and only the Mount Whitney intrusive suite reaches the high values of $(^{87}Sr/^{86}Sr)_i$ displayed by the intrusive suite of Yosemite Valley. A notable feature of the data set is that the mafic rocks from both the diorite of the Rockslides mafic complex (except leucocratic septa) and the mafic dikes on El Capitan have slightly higher $(^{87}Sr/^{86}Sr)_i$ ratios (0.7071–0.7072) and lower $\epsilon_{Nd}(t)$ values (–4.6 to −7.0) than the granites (0.7065–0.7066; −5.5 to −5.9). This trend is opposite to that observed in the nearby Tuolumne Intrusive Suite, for which the most silicic compositions have the most isotopically evolved compositions (Kistler et al., 1986; Coleman and Glazner, 1997). However, the range in isotopic variability across the compositional range of the intrusive suite of Yosemite Valley is still quite small (Fig. 11). Similar flat trends in initial isotopic compositions versus SiO_2 have been reported for plutonic rocks associated with the Lamarck Granodiorite (Coleman et al., 1992), the Goodale Canyon complex (Bradford, 1995), and the mafic complex at Onion Valley (Sisson et al., 1996). These trends contrast with the significant isotopic variation exhibited by the Fine Gold Intrusive Suite, whose $\epsilon_{Nd}(t)$ values span six units (Truschel, 1996), and by the Tuolumne Intrusive Suite, whose $\epsilon_{Nd}(t)$ values span seven units (Kistler et al., 1986; Coleman and Glazner, 1997).

In terms of Pb isotopes, plutonic rocks of the intrusive suite of Yosemite Valley plot at the radiogenic, upper end (high $^{206}Pb/^{204}Pb$) of the field for Sierra Nevada granitoids (Chen and Tilton, 1991). Like the Sr and Nd data, the Pb isotope data are fairly homogeneous (Fig. 12; representative data in Table 2) and are consistent with the Sr and Nd data in that the granitic rocks are slightly less radiogenic in composition (have lower $^{206}Pb/^{204}Pb$ ratios) than many of the mafic rocks associated with the intrusive suite of Yosemite Valley.

DISCUSSION

Emplacement of the Intrusive Suite of Yosemite Valley

Mafic-felsic interaction in the intrusive suite can be divided into two stages, early and late, on the basis of the crystallinity of the El Capitan Granite with which the mafic magmas came into contact. In the earlier stage, a partially molten El Capitan Granite carried and/or was invaded by abundant mafic magmas, which now form scattered enclaves, enclave swarms, small mafic pods, and the mafic complex represented by the diorite of the Rockslides mafic complex. Evidence of mafic-felsic mingling during this stage is provided by the leucocratic rocks (septa, stringers, and marginal sheaths) associated with the mafic rocks. Other workers have interpreted leucocratic septa as volumes of granitic mush that lost liquid by filter pressing after being trapped between mafic layers (e.g., Wiebe, 1993, 1996). Field and geochemical evidence (presented subsequently) support this conclusion for the origin of both the leucocratic septa within the diorite of the Rockslides mafic complex and the stringers within the mafic pods.

The later stage of mafic-felsic magmatism occurred after solidification of the El Capitan Granite and accompanied intrusion of the Taft Granite. The mafic magmas included in this stage are represented by the mafic dikes and planar enclave swarms exposed on El Capitan. Field and geochemical evidence (Reid et al., 1983; this work) suggests that these dikes partially melted solidified El Capitan Granite, producing hybrid rocks. In addition, field observations on the summit dome of El Capitan suggest that other hybrid rocks produced during this stage were probably a result of magma mingling and mixing between coeval mafic magma and Taft Granite.

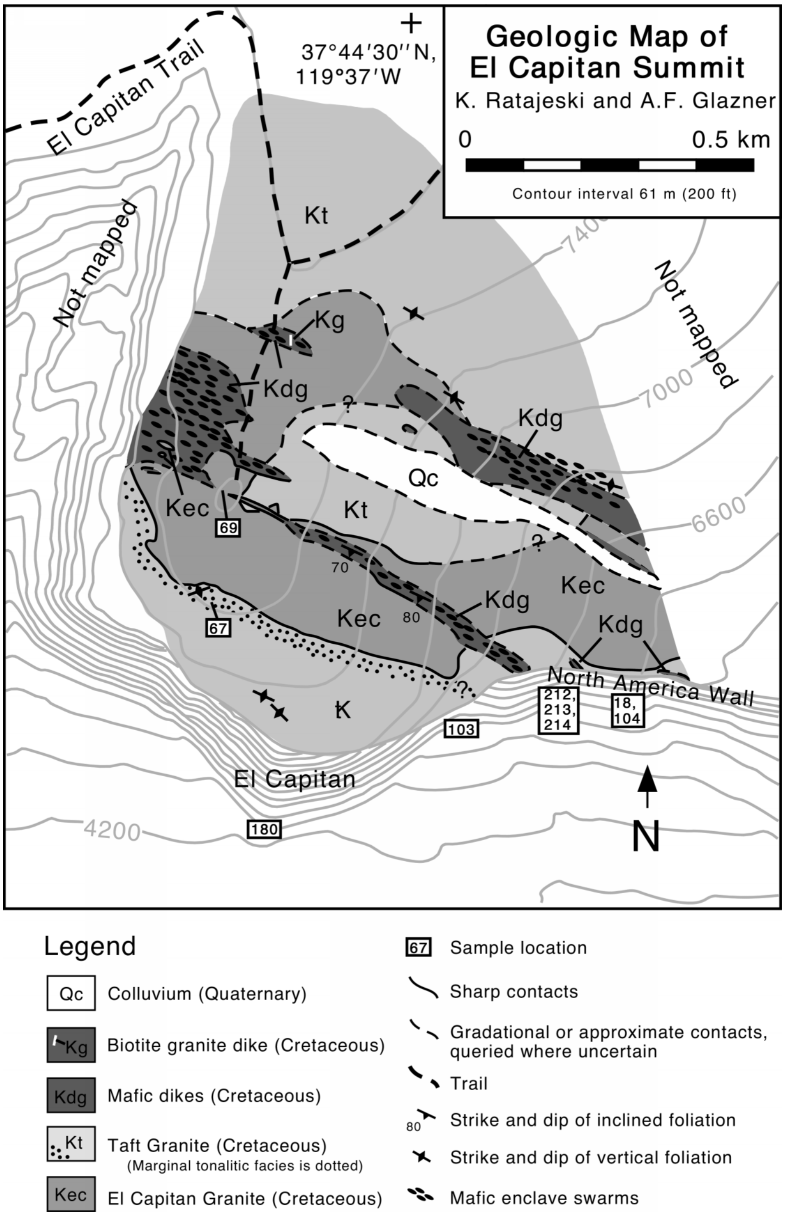

Figure 7. Geologic map of El Capitan summit.

Suite-Wide Trends

The nonlinear variations among the rocks of the intrusive suite of Yosemite Valley rule out large-scale magma mixing as an explanation for the chemical variation within the granites (sensu stricto), because the granites do not project toward likely coeval mafic liquids, particularly those represented by the chilled, fine-grained, mafic layers in the diorite of the Rockslides mafic complex (Fig. 9). Similarly, the highly scattered compositions of the mafic rocks defy a simple two-component mixing process involving a coeval granite magma such as the El Capitan or Taft Granite. It is likely therefore that some of the scatter among the mafic rocks results from crystal-liquid fractionation and/or more complex mixing behavior.

Granites

The mineralogic and isotopic similarity of the El Capitan and Taft Granites strongly suggests that these units are genetically related. The possibility that the variation within the granites represents varying degrees of partial melting from one homogeneous source is ruled out by the fact that the Taft Granite is the younger and more evolved of the two. The Taft may represent a smaller degree of partial melting of a similar source, partial melting of a more silicic source, or perhaps derivation by the separation of melt from early-formed solid phases within a crystalline mush of El Capitan Granite. A process of crystal-liquid fractionation may also be responsible for the chemical variation within the El Capitan Granite, which trends toward the Taft Granite on major element variation diagrams (Fig. 9) as well as on a modal plagioclase + biotite + (quartz + K-feldspar) diagram (Fig. 13).

Our attempts to model fractionation of low-

TABLE 1. U-Pb ZIRCON DATA

Sample number	Fraction (μm)	Description*	Grains (no.)	Mass (mg)	Total U (ppm)	Total Pb (ppm)	Comm Pb (pg)	$^{206}Pb^*/^{204}Pb$	$^{208}Pb/^{206}Pb$	$^{206}Pb/^{238}U$	Error (%)	$^{207}Pb/^{235}U$	Error (%)	$^{207}Pb/^{206}Pb$	Error (%)	$^{206}Pb/^{238}U$ age	$^{207}Pb/^{235}U$ age	$^{207}Pb/^{206}Pb$ age	Corr. coeff.
Taft Granite (YOS-1)																			
11	<74	White to clear, cracked prisms	89	0.089	6286.32	105.42	116.1	4945.70	0.156	0.016	0.10	0.10742	0.14	0.04869	0.09	102.3	103.6	133.0	0.744
12	<74	Yellow to clear prisms	69	0.071	4117.71	67.51	54.2	5574.62	0.123	0.016	0.11	0.10817	0.15	0.04864	0.10	103.1	104.3	130.5	0.737
El Capitan Granite (YOS-180)																			
15	>74	Heavily cracked prisms	41	0.200	1786.25	29.09	92.8	3999.08	0.117	0.016	0.25	0.10947	0.27	0.04890	0.10	103.8	105.5	143.1	0.928
16	>74	Heavily cracked prisms	54	0.308	1562.86	25.25	135.7	3637.99	0.118	0.016	0.20	0.10713	0.25	0.04856	0.13	102.3	103.3	126.5	0.839
17	>74	Heavily cracked prisms	8	0.006	2439.33	41.57	10.7	1436.05	0.169	0.016	0.16	0.10834	0.25	0.04829	0.19	104.1	104.4	113.3	0.662
18	>74	Heavily cracked prisms	6	0.006	4014.67	67.43	26.7	955.41	0.116	0.016	0.57	0.10887	0.61	0.04848	0.20	104.2	104.9	122.6	0.944
North America diorite (YOS-104)																			
10	<74	Acicular crystals	74	0.095	2220.34	38.29	53.4	4042.23	0.195	0.016	0.11	0.10732	0.15	0.04883	0.10	101.9	103.5	139.6	0.745
12	>74	Prismatic to acicular crystals	83	0.261	2601.10	46.20	71.8	9625.10	0.243	0.016	0.11	0.10650	0.15	0.04858	0.10	101.7	102.8	127.8	0.759
13	>74	Acicular crystals	51	0.184	1692.05	29.41	61.9	5134.87	0.210	0.016	0.11	0.10620	0.16	0.04841	0.11	101.8	102.5	119.3	0.733
14	>74	Prismatic to acicular crystals	8	0.010	2676.83	45.69	11.0	2470.47	0.200	0.016	0.11	0.10641	0.17	0.04860	0.12	101.6	102.7	128.4	0.704
15	>74	Prismatic to acicular crystals	7	0.020	2106.88	35.06	29.2	1486.70	0.139	0.016	0.34	0.10706	0.37	0.04863	0.13	102.1	103.3	130.2	0.933
16	>74	Prismatic to acicular crystals	8	0.020	1639.35	27.34	16.5	2052.08	0.156	0.016	0.43	0.10685	0.46	0.04826	0.16	102.7	103.1	112.0	0.940
Diorite of the Rockslides (YOS-23c)																			
16	>74	Prismatic to acicular crystals	43	0.128	251.71	4.45	16.3	2051.91	0.221	0.016	0.44	0.10733	0.47	0.04826	0.17	103.2	103.5	111.8	0.935
17	>74	Nonabraded prisms	59	0.034	2811.12	49.17	49.7	1984.10	0.196	0.016	0.17	0.10761	0.21	0.04881	0.12	102.3	103.8	138.7	0.833
Diorite of the Rockslides (YOS-206)																			
3	>74	Prisms	25	0.466	734.15	12.75	165.0	2125.61	0.189	0.016	0.15	0.10577	0.20	0.04825	0.13	101.7	102.1	111.7	0.755
9	>74	Equant crystals	29	0.183	417.94	6.82	75.3	1066.43	0.111	0.016	0.72	0.10791	0.75	0.04839	0.18	103.4	104.1	118.4	0.969
13	<74	Prismatic to acicular crystals	6†	0.021	667.59	10.65	6.6	2104.50	0.153	0.015	0.18	0.10292	0.21	0.04834	0.12	98.8	99.5	116.1	0.833
14	>74	Equant crystals and fragments	7†	0.056	968.96	16.51	11.5	4882.69	0.176	0.016	0.24	0.10735	0.25	0.04817	0.19	103.4	103.5	107.6	0.931
15b	>74	Slightly metamict fragments	3	0.024	1840.59	30.92	18.3	2514.31	0.148	0.016	0.25	0.10722	0.28	0.04811	0.11	103.4	103.4	104.9	0.918
16a	>74	Equant crystals	12	0.044	512.24	8.27	5.2	4522.30	0.112	0.016	0.13	0.10720	0.32	0.04804	0.29	103.5	103.4	101.2	0.419
16b	>74	Prismatic to equant crystals	14	0.084	427.62	7.1	17.6	2132.25	0.130	0.016	0.33	0.10688	0.67	0.04785	0.59	103.6	103.1	91.6	0.497

*Unless otherwise noted, all fractions consist of abraded zircons that are clear and free of cracks.
†Analyses performed at Syracuse University.

silica El Capitan Granite to produce Taft Granite liquid by simple models of fractional, equilibrium, and in situ crystallization were largely unsuccessful (Ratajeski, 1999). For a parental liquid, we used typical low-silica El Capitan Granite, and for a daughter liquid, we used typical Taft Granite. Because of the possibility that the magmas may have lost liquid by filter pressing during solidification, however, the use of common whole-rock compositions in the modeling is not without problems and may explain some of the negative results. Unambiguous samples of the original granitic liquids, such as might be found at quenched margins of dikes or plutons, were not identified in the intrusive suite of Yosemite Valley, and until they are, our hypothesis that the Taft and El Capitan Granites are genetically related remains untested.

Mafic and Associated Minor Leucocratic Rocks

Some of the scatter among the mafic rocks on the major element diagrams may be attributed to the fact that some of these samples are cumulates, but distinguishing liquid compositions from cumulates is difficult except for the most obvious cases. For example, diorite of the Rockslides mafic complex sample YOS-95b, interlayer leucocratic septum YOS-55b, and marginal sheath YOS-103b all have elevated modal plagioclase and high Al_2O_3, suggesting that they are partly composed of cumulate plagioclase. Obvious hornblende cumulates are generally lacking from the data set, as no samples greatly depart from the chilled mafic layers (representing the original liquids) toward the hornblende apex on modal plagioclase + hornblende + biotite diagrams (Fig. 13). Except for the plagioclase cumulates in rocks at mafic-felsic contacts, obvious cumulates are few, and we conclude that extreme crystal fractionation is not a common feature within the mafic rocks associated with the intrusive suite of Yosemite Valley.

Evidence for the trapping of volumes of coeval granitic material within the diorite of the Rockslides mafic complex is provided by the leucocratic interlayer septa. On a modal plagioclase + biotite + (quartz + K-feldspar) ternary diagram, these rocks, along with other leucocratic samples from stringers and marginal sheaths around mafic pods, define a linear array that projects away from the quartz + K-feldspar apex, almost reaching the mafic end of the range displayed by the El Capitan Granite (Fig. 13). These rocks probably represent partially crystalline El Capitan Granite magma that was trapped during injection of

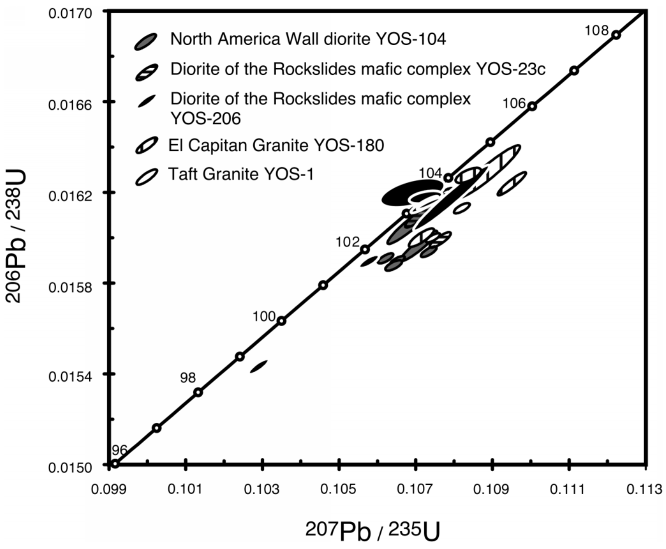

Figure 8. U-Pb concordia diagram. Concordia is graduated in million years, and error ellipses are two standard deviations. None of the discordant data are sufficiently aligned to construct discordia.

mafic magmas at the base of a magma chamber (Wiebe, 1993, 1996). Bulk mixing between mafic liquids (modeled by the fine-grained mafic layers) and felsic liquids (modeled by samples of El Capitan Granite) does not produce the compositions of the leucocratic septa or the marginal sheaths. Rather, the linear trend on the modal diagram probably reflects some combination of (1) loss of silicic melt by filter pressing prior to or during injection and compaction of the mafic layers, (2) selective exchange of mobile alkalis between the felsic and mafic magmas (Wiebe, 1996), and (3) varying degrees of mafic component acquired during mingling. The cumulate nature of these rocks is suggested by their elevated Sr contents (which is compatible in plagioclase), yet these rocks also preserve an enriched LREE signature, possibly indicating that filter pressing took place in the presence of LREE-rich trace phases, which remained behind in the solid residue. This idea is supported by the identification of abundant apatite, sphene, and allanite within interlayer septa samples YOS-105b and YOS-109b.

The origin of the mafic dikes on El Capitan can be addressed with the major and trace element data. On the basis of field observations and major element geochemistry, Reid et al. (1983) hypothesized that mixing of mafic magmas similar to those of the North America dikes with alaskitic partial melts of El Capitan Granite host rock could explain the origin of the biotite-rich, ''pre–North America Wall'' dikes of the first injection phase. Our major element data are consistent with this interpretation, but our limited REE analyses indicate that if this mixing process occurred, it did not result in rocks with REE patterns intermediate between the mafic and felsic end members of the suite: among the two pre–North America dikes sampled, one has an elevated LREE signature similar to the granites, and one has a less enriched signature similar to the diorite of the Rockslides mafic complex and North America dikes (Fig. 10). The REE data suggest that while El Capitan Granite was interacting with the margins of the dike complex, it retained most of its REEs (probably in unmelted trace phases) and therefore did not contribute a large amount of REEs to the partial melts, which consequently mixed with the mafic magmas. Similarly, interaction of North America mafic dikes with Taft Granite on the summit dome of El Capitan also did not result in rocks with intermediate REE patterns: our single analysis of biotite tonalite YOS-67 results in LREE values as enriched as most El Capitan and Taft Granite samples. As for other petrologic processes, evidence for minor crystal fractionation within the North America dike complex is not very great, as only one anomalously hornblende-rich sample (YOS-214) is present in the data set.

Petrogenesis

Perhaps the most striking aspect of the geochemical data is the rather small amount of isotopic variability that characterizes the intrusive suite of Yosemite Valley across its entire petrologic range. Coleman et al. (1992) and Coleman and Glazner (1997) have interpreted isotopic variations within intrusive suites of the Sierra Nevada as reflecting different roles of ancient continental crust. For suites that show significant isotopic contrast as well as inheritance in zircon systematics (e.g., Tuolumne), the involvement of significant amounts of preexisting, ancient crust is implicated. In contrast, a relatively small role for preexisting crust is implicated for isotopically homogeneous suites with few inherited zircons. Coleman et al. (1992) raised the possibility that most of the Lamarck Granodiorite could have been extracted relatively rapidly from an enriched mantle source with ($^{87}Sr/^{86}Sr)_i$ ratios of ~0.7065 and $\epsilon_{Nd}(t)$ of ~−4.5. Granitic rocks of the intrusive suite of Yosemite Valley have essentially this composition, which permits a similar source. However, as noted by other workers (Ben Othman et al., 1989; Beard and Johnson, 1997), Sr and Nd isotopes are often not sufficient to distinguish among the various processes that can result in enriched isotopic compositions, e.g., crustal contamination of mantle magmas, mantle enrichment by sediment subduction, and foundering of crustal rocks into the mantle (e.g., Beard and Glazner, 1995).

In Figure 12, we plot several compositional fields representing Pb isotope reservoirs that may have been relevant to the genesis of the intrusive suite of Yosemite Valley, including subducted marine sediments, ancient metasedimentary rocks, and enriched lithospheric mantle. Pb isotope compositions of intrusive suite rocks are far removed from those of marine sediments, suggesting that subducted sediments are not a likely source for Pb in the intrusive suite. In contrast, ancient metasedimentary Pb is a more likely component in the intrusive suite samples, as most of the samples fall within or close to the Type II Pb province of Zartman (1974), a region that spans much of north-central Nevada and contains great thicknesses of miogeoclinal sedimentary rocks derived from Precambrian sources.

Whether this metasedimentary component was added by contamination of mantle-derived magmas (perhaps within the lower crust) or by direct contamination of the upper mantle itself (by foundering of crustal rocks into the mantle at some time in the remote past) is unknown, but the fact that the Sr, Nd, and Pb isotope compositions become less crust-like with increasing SiO_2 argues against contamination of primitive mafic magmas by a high-silica, ancient crustal component. The western Yosemite Valley plutonic rocks are just above the upper $^{206}Pb/^{204}Pb$ limit of the field for the Western Great Basin basalts (Beard and John-

TABLE 2. GEOCHEMICAL DATA FOR SELECTED SAMPLES

	El Capitan Granite		Taft Granite		Rocks associated with mafic pods			Diorite of the Rockslides			"Pre–North America Wall" dikes		"North America Wall" dikes	
	Low-silica	High-silica	Low-silica	High-silica	Diorite	Leucocratic stringer	Marginal sheath	Mafic layer	Interlayer septum	Leucocratic diorite	Enclave in dike	Enclave matrix	Diorite	Hornblende cumulate?
	YOS-61	YOS-103c	YOS-1	YOS-210	YOS-103a	YOS-82b	YOS-103b	YOS-55a	YOS-105b	YOS-206	YOS-18c	YOS-18a	YOS-104	YOS-214
SiO_2	71.27	73.49	73.28	76.23	53.13	65.17	60.75	53.47	64.73	56.90	55.61	68.05	57.59	50.55
TiO_2	0.37	0.22	0.10	0.04	1.31	0.71	0.67	1.02	0.78	0.77	1.18	0.62	0.96	1.61
Al_2O_3	14.87	14.12	14.79	13.28	17.77	17.36	20.03	17.69	17.53	17.46	17.09	15.79	17.01	16.91
Fe_2O_3*	3.10	2.08	1.24	0.68	9.44	4.59	5.04	8.94	4.69	4.81	8.65	4.30	7.61	12.54
MnO	0.07	0.05	0.04	0.02	0.14	0.05	0.07	0.15	0.04	0.16	0.18	0.04	0.13	0.15
MgO	0.89	0.52	0.16	0.07	4.47	1.63	1.50	5.38	1.49	8.14	4.14	1.65	4.10	5.50
CaO	2.50	1.98	1.21	1.02	8.43	4.81	4.87	9.24	5.31	6.88	7.52	4.08	7.72	9.34
Na_2O	3.85	3.69	3.48	3.16	3.33	3.45	4.76	2.72	3.62	2.65	3.49	3.56	2.98	2.40
K_2O	2.99	3.80	5.65	5.48	1.69	2.01	2.10	1.18	1.51	2.09	1.83	1.79	1.66	0.85
P_2O_5	0.11	0.06	0.05	0.03	0.27	0.22	0.22	0.21	0.31	0.13	0.30	0.11	0.22	0.14
Total	101.09	100.64	98.05	99.25	99.93	101.11	100.72	99.77	100.40	99.09	100.44	101.57	98.22	101.04
LOI	0.63	0.40	0.37	0.40	0.84	0.53	0.63	1.40	0.47	0.97	0.64	0.50	0.69	0.75
Ba	1397	782	1219	458	512	880	910	435	900	738	635	770	608	339
Cr	10	9	6	2	49	10	13	98	10	24	17	17	55	18
Ni	N.D.	N.D.	N.D.	4	21	5	8	39	6	22	9	9	25	19
Sc	6	4	3	5	23	9	8	26	7	17	7	7	18	26
Sr	311	236	175	134	503	569	575	466	812	518	472	466	446	495
V	43	23	3	9	205	72	62	193	71	137	197	75	158	438
Y	17	11	11	3	29	15	15	18	12	15	26	12	19	25
Zr	212	103	162	26	189	243	311	129	274	79	275	197	209	139
Rb	92.4	N.D.	148.9	N.D.	64.8	N.D.	99.1	29.5	53.1	N.D.	122.4	84.0	50.0	N.D.
Sr	299.7	N.D.	168.5	N.D.	479.8	N.D.	558.1	457.0	772.2	N.D.	453.2	438.8	453.4	N.D.
$^{87}Rb/^{86}Sr$	0.8908	N.D.	2.5561	N.D.	0.3908	N.D.	0.5135	0.1869	0.1989	N.D.	0.7812	0.5537	0.3188	N.D.
$^{87}Sr/^{86}Sr$	0.707871	N.D.	0.710289	N.D.	0.708301	N.D.	0.707679	0.707450	0.706982	N.D.	0.707993	0.707690	0.707555	N.D.
$(^{87}Sr/^{86}Sr)_i$	0.706567	N.D.	0.706548	N.D.	0.707729	N.D.	0.706927	0.707176	0.706691	N.D.	0.706849	0.706880	0.707089	N.D.
Sm	4.35	N.D.	3.17	N.D.	4.76	N.D.	3.41	3.69	5.26	N.D.	4.90	3.37	7.48	N.D.
Nd	27.42	N.D.	19.43	N.D.	22.48	N.D.	18.23	17.45	38.77	N.D.	23.71	26.31	21.19	N.D.
$^{147}Sm/^{144}Nd$	0.0982	N.D.	0.1009	N.D.	0.1311	N.D.	0.1157	0.1308	0.0839	N.D.	0.12793	0.0793	0.2186	N.D.
$^{143}Nd/^{144}Nd$	0.512346	N.D.	0.512337	N.D.	0.512279	N.D.	0.512337	0.512321	0.512333	N.D.	0.512316	0.512322	0.512334	N.D.
$\epsilon_{Nd}(t)$	–4.40	N.D.	–4.62	N.D.	–6.14	N.D.	–4.80	–5.30	–4.46	N.D.	–5.38	–4.62	–6.22	N.D.
$^{208}Pb/^{204}Pb$	19.256	N.D.	N.D.	N.D.	38.974	N.D.	38.913	N.D.	19.329	39.006	38.897	N.D.	38.917	N.D.
$^{207}Pb/^{204}Pb$	15.694	N.D.	N.D.	N.D.	15.717	N.D.	15.702	N.D.	15.689	15.730	15.694	N.D.	15.702	N.D.
$^{208}Pb/^{204}Pb$	38.884	N.D.	N.D.	N.D.	38.974	N.D.	38.913	N.D.	38.876	39.006	38.897	N.D.	38.917	N.D.

Note: Major element compositions are in weight percent; trace element compositions are in parts per milion. Major elements compositions express total Fe as Fe_2O_3 and have been normalized 100 wt% anhydrous. Typical standard errors ($s_i/\sqrt{n}$, in wt%) for the major element analyses are SiO_2, 0.29; TiO_2, 0.01; Al_2O_3, 0.06; Fe_2O_3t, 0.06; MnO, 0.00; MgO, 0.02; CaO, 0.05; Na_2O, 0.03; K_2O, 0.03; P_2O_5, 0.01. Reported totals are original analysis totals. LOI—loss on ignition (in wt%). N.D.—not determined. Rb, Sr, Sm, and Nd data are from whole-rock samples. Pb data are from feldspar separates.

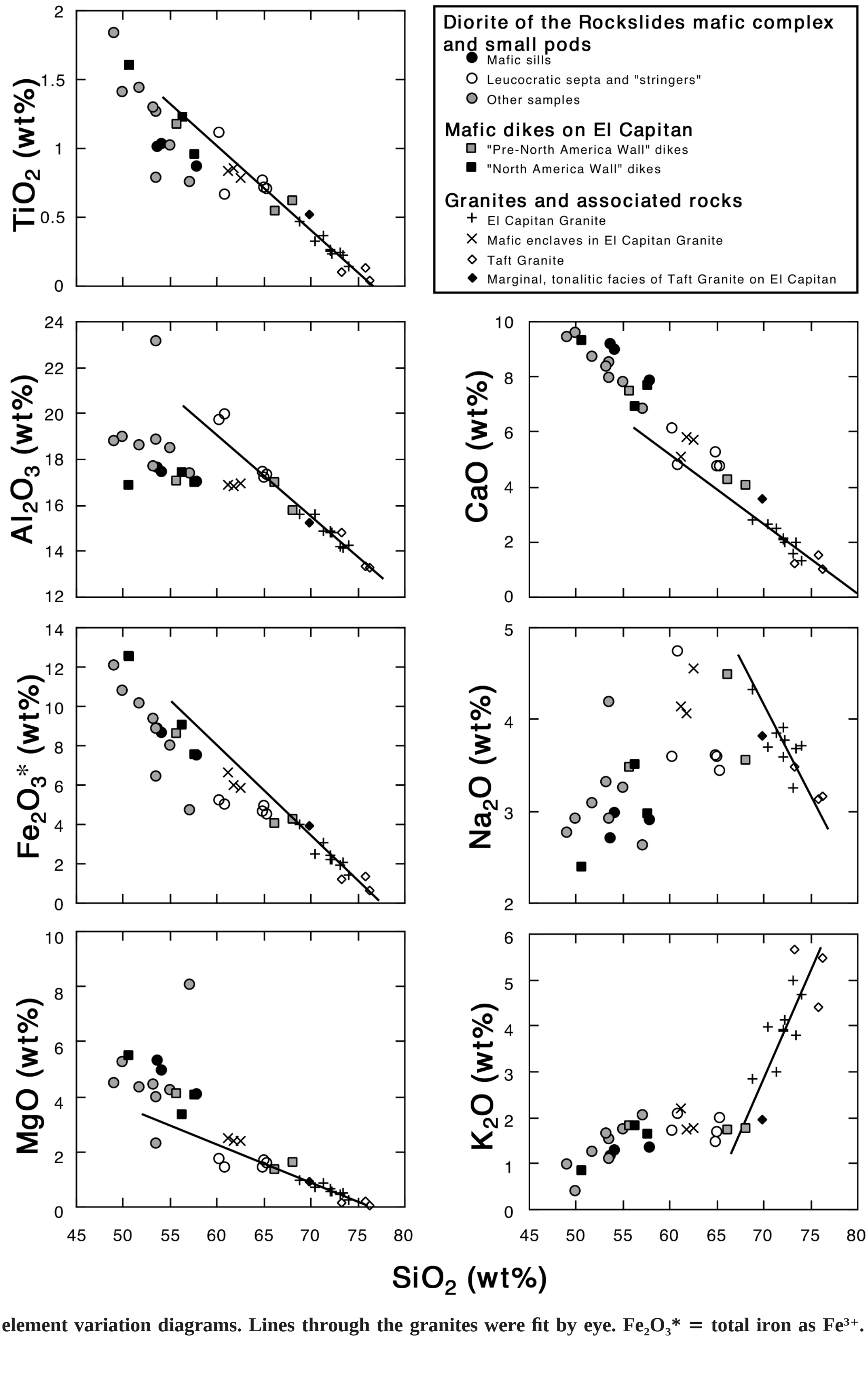

Figure 9. Major element variation diagrams. Lines through the granites were fit by eye. $Fe_2O_3^*$ = total iron as Fe^{3+}.

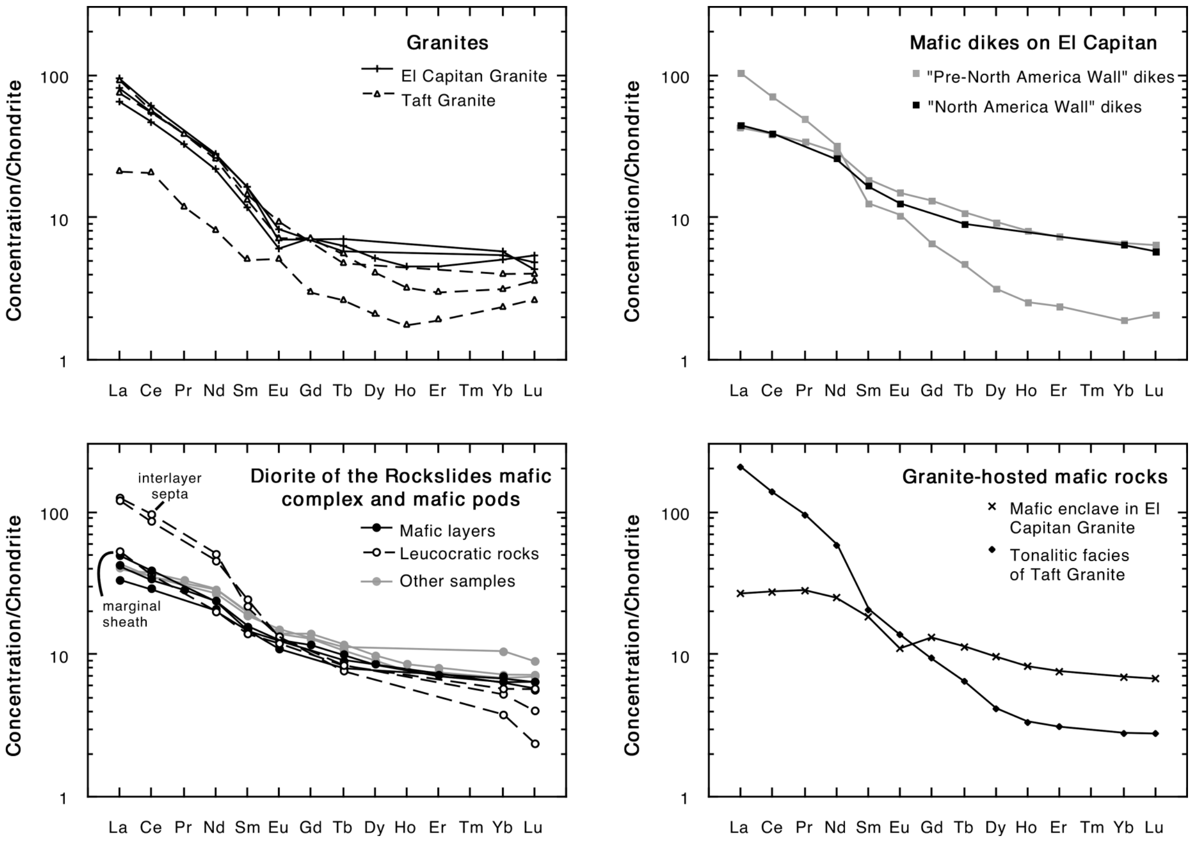

Figure 10. REE concentrations normalized to chondritic values (Anders and Grevesse, 1989). Note that this figure plots both INAA and ICP-MS data; the same REEs were not analyzed by both methods.

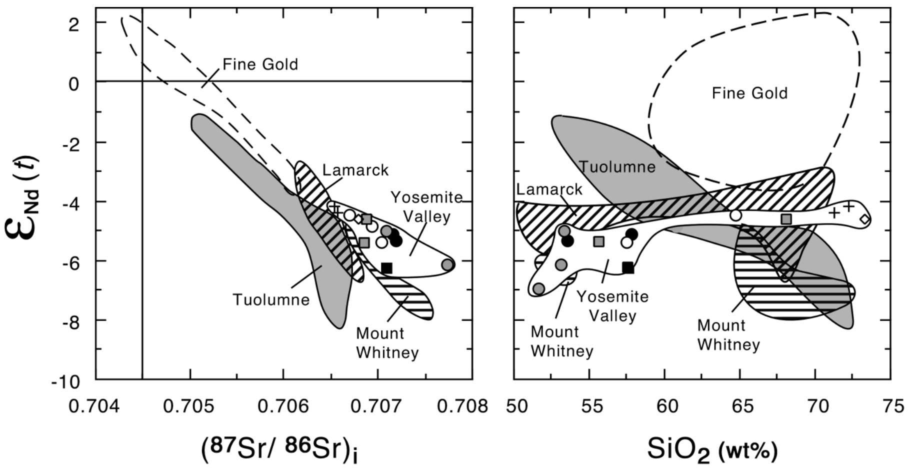

Figure 11. Initial Sr and Nd isotope compositions of plutonic rocks from the western half of Yosemite Valley compared with those of other intrusive suites from the central Sierra Nevada batholith. All data are corrected for 103 m.y. of radiogenic growth (based on the age determined by Stern et al., 1981). Symbols for the data from the intrusive suite of Yosemite Valley are the same as those in Figure 9. Data sources for the other intrusive suites are as follows: Fine Gold Intrusive Suite (Truschel, 1996), Lamarck Granodiorite (Coleman et al., 1992), Tuolumne Intrusive Suite (Kistler et al., 1986; Coleman and Glazner, 1997), and Mount Whitney Intrusive Suite (Hirt and Glazner, 1995).

son, 1997), which, along with ultrapotassic basaltic lavas in the Sierran region (Van Kooten, 1981), are believed to have originated from an enriched, lithospheric mantle (Ormerod et al., 1988; Menzies, 1989). The isotopic proximity of the western Yosemite Valley plutonic rocks and the Western Great Basin basalts may hint at an enriched-mantle component in the granites and gabbros of the intrusive suite of Yosemite Valley, and involvement of metasedimentary Pb in this process would seem to be implicated by the Pb isotope data.

The broad isotopic similarity between the Yosemite Valley granites and mafic rocks suggests that these rock types are related petrogenetically. One possibility that is consistent with the geochemical data is that a parental, granodioritic melt (e.g., a melt similar in composition to YOS-61) was produced by partial melting of relatively young, LILE-enriched mafic rocks in the lower crust (Fig. 14). Because the El Capitan Granite is associated with coeval gabbroic rocks (mafic enclaves, mafic pods, and the diorite of the Rockslides), it is conceivable that the intrusion of the mafic magma caused the partial melting event that

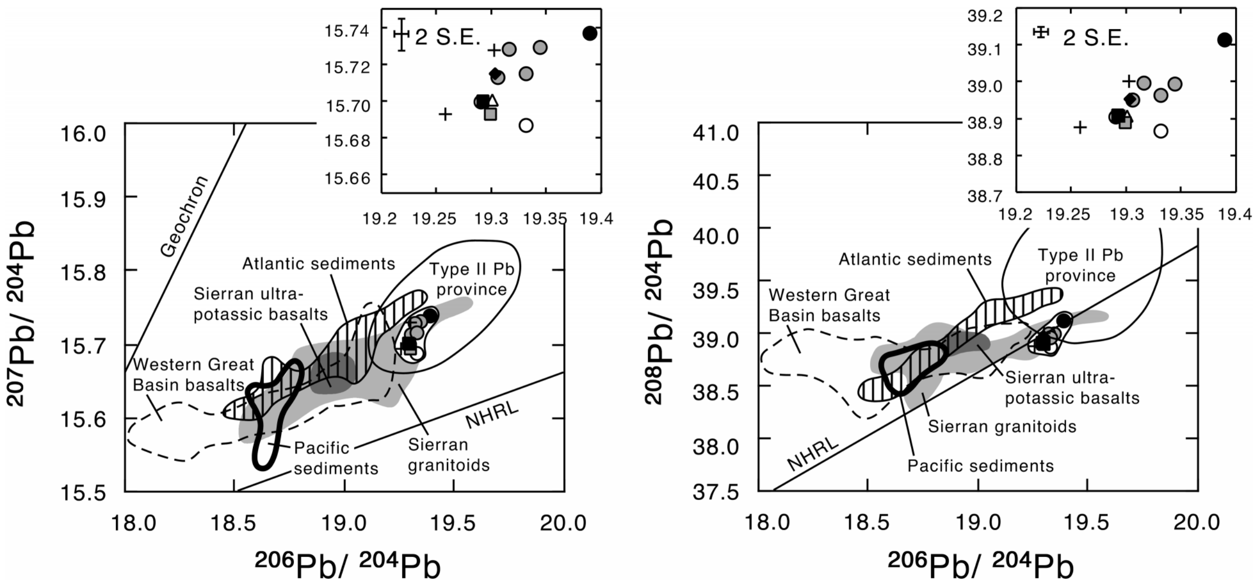

Figure 12. Pb isotope data for feldspars from plutonic rocks associated with the intrusive suite of Yosemite Valley. Symbols are the same as those in Figure 9; the additional open triangle represents a foliated, leucocratic quartz diorite collected from the contact between the El Capitan Granite and the diorite of the Rockslides mafic complex. Reference lines shown on the diagrams are the present-day geochron (Tatsumoto et al., 1973) and the Northern Hemisphere reference line (NHRL) of Hart (1984), which is regressed through mid-ocean ridge basalt (MORB) and oceanic-island basalt (OIB) data. The field for granitoids of the central Sierra Nevada batholith (Chen and Tilton, 1991) includes data only from feldspar separates, which are uncorrected for minor U decay to correspond with our data. Also shown for reference are the fields for modern marine sediments in the Pacific and Atlantic Oceans (Ben Othman et al., 1989), the Type II Pb isotope province of Zartman (1974), which is thought to reflect sources associated with Precambrian metasedimentary rocks, and the fields for ultrapotassic basalts of the central Sierra Nevada (Van Kooten, 1981) and basalts from the western Great Basin (Beard and Johnson, 1997), both of which are thought to originate from the lithospheric mantle. Two-standard-error uncertainties are from the analysis of standard NBS 981.

Figure 13. Modal variations (in wt%). Modal data plotted in this figure were estimated by least-squares mass balance of bulk compositions against phase compositions determined by microprobe for representative samples (Table DR6 in GSA Data Repository; see text footnote 1). The quartz-poor mafic rocks are plotted on the hornblende-plagioclase-biotite ternary diagram (projected from quartz), and the hornblende-free leucocratic rocks (including granites) are plotted on the plagioclase–biotite–(quartz + K-feldspar) ternary diagram. Compositions of mafic enclaves within the El Capitan Granite are not plotted because they have significant amounts of both quartz and hornblende.

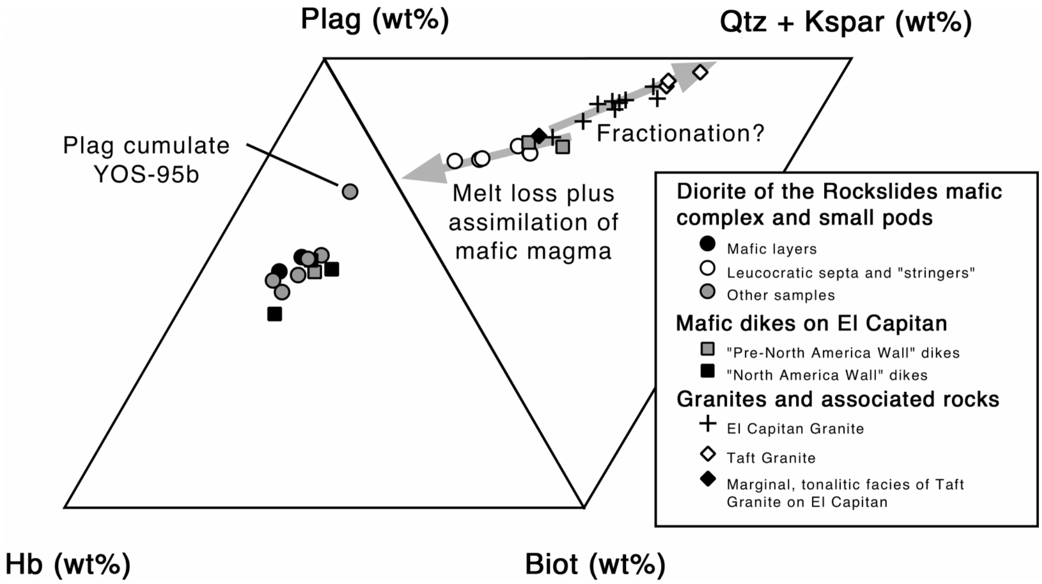

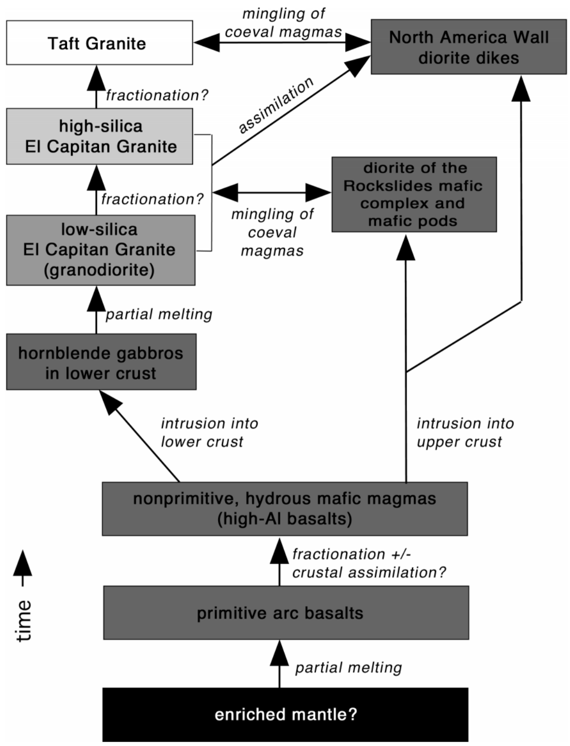

Figure 14. Petrogenetic model for the intrusive suite of Yosemite Valley.

in turn produced the granite. Experimental partial melting of a hornblende gabbro from the diorite of the Rockslides mafic complex at 800–825 °C and 8 kbar (with no added fluid) produces partial melts similar in composition to low-silica El Capitan Granite (Ratajeski and Sisson, 1999), a preliminary finding that lends support to the model just outlined.

As shown by Coleman et al. (1992), the Lamarck Granodiorite provides a similar example of isotopic near-homogeneity among coeval mafic and felsic plutonic rocks. The isotopic composition of the Lamarck is very similar to that of the intrusive suite of Yosemite Valley (Fig. 11), which raises the possibility of a similar source for both intrusive suites. However, there is an important difference between the two suites: the Lamarck contains large amounts of intermediate magma (granodiorite), which appears to have been produced by mixing of mafic and felsic magmas at a fairly early or deep stage (Frost and Mahood, 1987; G. Mahood, 2000, personal communication). A later stage of mafic-felsic magmatism produced several small mafic plutons, which are locally mingled with the Lamarck Granodiorite, but on the whole are still largely unhybridized with it. This later stage of mafic-felsic magmatism is very similar to that inferred for the intrusive suite of Yosemite Valley, during which coeval mafic and felsic components remained largely unhybridized. The record of mafic-felsic magmatism in the intrusive suite of Yosemite Valley and other complexes in the Sierra Nevada underscores the considerable variability in the spatial and temporal scales of mafic-felsic interaction within arcs.

CONCLUSIONS

1. The intrusion of the Yosemite Valley suite involved two probably closely timed pulses of mafic-felsic magmatism. The first stage yielded the El Capitan Granite and mafic magmas that comprise scattered enclaves, enclave swarms, small pods, and the diorite of the Rockslides mafic complex. The second stage yielded the Taft Granite and the mafic dike swarm exposed on El Capitan.

2. Mingling of mafic and felsic magmas has produced biotite-rich, leucocratic quartz diorites to tonalites, which form thin septa between mafic layers in the diorite of the Rockslides mafic complex, irregular masses within mappable pods of mafic rocks, and contact zones between mafic rocks and the El Capitan Granite. Modal and geochemical data suggest that some of these leucocratic rocks are plagioclase-rich cumulates. On the North America Wall of El Capitan, some areas of the El Capitan Granite interacted with a large mafic dike complex and partially melted but at low-enough temperatures to prevent REE mobilization into adjacent mafic magmas.

3. Initial isotopic compositions of the mafic and felsic rocks are very similar; the mafic rocks exhibit only slightly more enriched compositions than the granites. This observation argues against contamination of unevolved mafic magmas by ancient continental crust, but could be reconciled with a two-stage process whereby melting of an enriched mantle (perhaps enriched by foundering of ancient continental crust) produced mafic rocks, which were remelted a short time later during a subsequent pulse of mafic magmatism.

APPENDIX 1. ANALYTIC METHODS: U-Pb ZIRCON GEOCHRONOLOGY

Zircons were separated, picked, abraded, and dissolved by standard techniques, a mixed ^{205}Pb-^{233}U-^{236}U spike was added, and then Pb and U were collected by standard HBr column chemistry. Total procedural blanks were 2–18 pg Pb and <1 pg U. Pb and U isotope ratios for all but two of the picked fractions were determined with the VG Sector 54 mass spectrometer at the University of North Carolina (UNC) at Chapel Hill. Both U and Pb analyses were conducted in static collection mode, using all Faraday detectors for U and combined Faraday (^{205}Pb, ^{206}Pb, ^{207}Pb, and ^{208}Pb) and Daly (^{204}Pb) detectors for Pb. Long-term repeat measurements of NBS 981 ($n = 32$; errors are 1 S.D.) yield $^{206}Pb/^{204}Pb = 16.937 \pm 0.16\%$, $^{207}Pb/^{204}Pb = 15.48 \pm 0.16\%$, $^{208}Pb/^{204}Pb = 36.69 \pm 0.17\%$, $^{207}Pb/^{206}Pb = 0.9147 \pm 0.044$, and $^{208}Pb/^{206}Pb = 2.167 \pm 0.064$. Data obtained at UNC were corrected for fractionation of 0.12% ± 0.08%/amu (atomic mass unit; Faraday) and 0.20% ± 0.07%/amu (Daly). As an independent check on the accuracy of the UNC analyses, two fractions (YOS-206–13 and YOS-206–14) were prepared at UNC but analyzed with the VG Sector 54 mass spectrometer at Syracuse University and corrected for fractionation of 0.18% ± 0.07%. Raw data were reduced with the Pb MacDat–2 program (D. Coleman, 1999, personal commun.) using data-reduction and error-propagation algorithms of Ludwig (1989, 1990). Concordia plots, age estimates, and age errors were generated with a recently updated version of the Isoplot program (Ludwig, 1990).

APPENDIX 2. ANALYTIC METHODS: WHOLE-ROCK GEOCHEMISTRY

Only fresh samples were chosen for whole-rock geochemical analysis. Major elements (Si, Ti, Al, Fe, Mn, Mg, Ca, Na, K, and P) and trace elements (Ba, Cr, Ni, Sc, Sr, V, Y, and Zr) were measured by direct current plasma–atomic emission spectrometry (DCP-AES) for crushed powders of representative samples of the main rock types described herein, using the method outlined by Beard and Glazner (1995). Rb analyses were attempted along with the other trace elements by DCP-AES, but flat calibration curves (small signal to concentration ratio) did not permit accurate analyses. Mafic samples were generally run separately from felsic samples. Calibration curves were calculated for each run by analyzing several standards spanning the expected concentration range of the unknowns. For runs consisting of mafic samples, standards included five of the following: AGV-1, BIR-1, DNC-1, MAG-1, SDC-1, and STM-1. For runs analyzing intermediate to silicic rocks, standards included granite standard G-2 and/or rhyolite standard RGM-1, plus four standards from the preceding list. Along with one of the standards, each sample was analyzed several times (three to four times for major elements and four times for trace elements), accounting for instrumental drift, and means and standard deviations were computed after anomalous data points were discarded. The whole-rock major element data were used in conjunction with microprobe analyses of constituent phases to determine precise modal abundances by mass balance.

Trace element concentrations were also obtained for several samples by instrumental neutron activation analysis (INAA) at Oregon State University and by inductively coupled plasma–mass spectrometry (ICP-MS) at Duke University. Multiple elements (including REEs) were analyzed by these methods. The reproducibility of the ICP-MS analyses, as judged by replicate dissolutions, is $\pm$1%–3% for REE and $\pm$1%–6% for other elements (Klein and Karsten, 1995). ICP-MS analyses of Zr and Hf resulted in extremely depleted concentrations in standard G-2 relative to their accepted concentrations, an effect that probably resulted from incomplete dissolution of minor, refractory, trace element–rich phases like zircon. As a result, Zr and Hf data by ICP-MS are not included in this study. One-standard-deviation uncertainties for the INAA analyses are generally less than 10%.

Rb, Sr, Sm, and Nd isotope compositions were obtained for selected whole-rock samples, and Pb isotopes were obtained from feldspar separates, by using the techniques described by Miller et al. (1995) and Fullagar et al. (1997). All isotopic analyses were performed with the eight-collector VG Sector 54 mass spectrometer at the University of North Carolina. Sr isotope compositions were normalized to $^{86}Sr/^{87}Sr = 0.1194$ by using an exponential fractionation law and referenced to NBS 987 for which $^{87}Sr/^{86}Sr = 0.710\,250$. Nd isotope compositions are normalized to $^{146}Nd/^{144}Nd = 0.7219$ by using an exponential fractionation law and referenced to UNC Ames Nd metal with $^{143}Nd/^{144}Nd = 0.512\,14$. Replicate analyses of NBS 987 run during the sample analyses gave $^{87}Sr/^{86}Sr = 0.710\,340$ ($\pm$ 0.000 022; two standard errors; $n = 4$). Replicate analyses of UNC Ames gave $^{143}Nd/^{144}Nd = 0.512\,143$ ($\pm$ 0.000 0078; two standard errors; $n = 2$). Long-term, internal run precision for Sr and Nd analyses at UNC is better than 0.0010% ($\pm$ 0.000 007 for Sr and $\pm$ 0.000 005 for Nd). Measured $^{87}Sr/^{86}Sr$ ratios were corrected for 103 m.y. of radiogenic growth, based on the age of the El Capitan Granite as determined by Stern et al. (1981). If the discordance of our preliminary zircon results is due to Pb loss (see earlier discussion), rocks of the intrusive suite of Yosemite Valley may be slightly older, i.e., their ages may be as great as 110–115 Ma. This change is not very significant for the initial $^{87}Sr/^{86}Sr$ calculation, however, and results in an increase of only 0.0001. For the Pb isotope analyses, total procedural blank was 96 pg Pb, and analyses were referenced to NBS 981 with $^{207}Pb/^{206}Pb = 0.914\,64$ and corrected 0.086 $\pm$ 0.009%/amu for fractionation. Average uncertainties (two standard errors; $n = 44$) for the analyzed samples due to measurement uncertainty and propagation through the fractionation correction are 0.0012 for $^{206}Pb/^{204}Pb$, 0.012 for $^{207}Pb/^{204}Pb$, and 0.018 for $^{208}Pb/^{204}Pb$.

ACKNOWLEDGMENTS

This work was partly supported by National Science Foundation grants 9219521 and 9526803 (to Glazner) and additional funding from Sigma Xi, the Geological Society of America, and the University of North Carolina Department of Geological Sciences. Field assistance by Jennifer Wenner and William Hoyt is much appreciated. Discussions in the field with John Bartley, Mark Brandon, David Hawkins, Tom Sisson, and Robert Wiebe are much appreciated. Paul Fullagar, Kevin Stewart, James Beard, and Peter Malin are thanked for early reviews of this paper; reviews by Gail Mahood, Brendan McNulty, and Robert Wiebe greatly improved the revised version. We thank Scott Samson and Greg Wortman at the Syracuse University geochronology laboratory for analyses of two zircon fractions. Whole-rock INAA data were provided by the U.S. Department of Energy's Reactor Sharing Grant to Oregon State University. Finally, Ratajeski was supported by a National Science Foundation Graduate Research Fellowship.

REFERENCES CITED

Allègre, C.J., and Othman, D.B., 1980, Nd-Sr isotopic relationship in granitoid rocks and continental crust development: A chemical approach to orogenesis: Nature, v. 286, p. 335–342.

Anders, E., and Grevesse, N., 1989, Abundances of the elements: Meteoritic and solar: Geochimica et Cosmochimica Acta, v. 53, p. 197–214.

Barbarin, B., 1990, Plagioclase xenocrysts and mafic magmatic enclaves in some granitoids of the Sierra Nevada batholith, California: Journal of Geophysical Research, v. 95, p. 17 747–17 756.

Bateman, P.C., 1992, Plutonism in the central part of the Sierra Nevada batholith, California: U.S. Geological Survey Professional Paper 1483,186 p.

Bateman, P.C., and Chappell, B.W., 1979, Crystallization, fractionation, and solidification of the Tuolumne Intrusive Series, Yosemite National Park, California: Geological Society of America Bulletin, v. 90, p. 465–482.

Beard, B.L., and Glazner, A.F., 1995, Trace element and Sr and Nd isotopic compositions of mantle xenoliths from the Big Pine volcanic field, California: Journal of Geophysical Research, v. 100, p. 4169–4179.

Beard, B.L., and Johnson, C.M., 1997, Hafnium isotope evidence for the origin of Cenozoic basaltic lavas from the southwestern United States: Journal of Geophysical Research, v. 102, p. 20 149–20 178.

Ben Othman, D., White, W.M., and Patchett, J., 1989, The geochemistry of marine sediments, island arc magma genesis, and crust-mantle recycling: Earth and Planetary Science Letters, v. 94, p. 1–21.

Bergantz, G.W., 1989, Underplating and partial melting: Implications for melt generation and extraction: Science, v. 245, p. 1093–1095.

Bowen, N.L., 1928, The evolution of the igneous rocks: Princeton, New Jersey, Princeton University Press, 332 p.

Bradford, K.J., 1995, Petrology of a mafic intrusive suite in the central Sierra Nevada batholith, California [M.S. thesis]: Chapel Hill, University of North Carolina, 277 p.

Calkins, F.C., 1930, The granitic rocks of the Yosemite region, *in* Matthes, F.E., Geologic history of the Yosemite Valley: U.S. Geological Survey Professional Paper 160, p. 120–129.

Calkins, F.C., Huber, N.K., and Roller, J.A., 1985, Geologic bedrock map of Yosemite Valley, Yosemite National Park, California: U.S. Geological Survey Map I-1639, 1 sheet, scale 1:24 000.

Castro, A., Moreno-Ventas, I., and de la Rosa, J.D., 1991, H-type (hybrid) granitoids: A proposed revision of the granite-type classification system and nomenclature: Earth-Science Reviews, v. 31, p. 237–253.

Chen, J.H., and Tilton, G.R., 1991, Applications of lead and strontium isotopic relationships to the petrogenesis of granitoid rocks, central Sierra Nevada batholith, California: Geological Society of America Bulletin, v. 103, p. 439–447.

Coleman, D.S., and Glazner, A.F., 1997, The Sierra crest magmatic event: Rapid formation of juvenile crust during the Late Cretaceous in California: International Geology Review, v. 39, p. 768–787.

Coleman, D.S., Frost, T.P., and Glazner, A.F., 1992, Evidence from the Lamarck Granodiorite for rapid Late Cretaceous crust formation in California: Science, v. 258, p. 1924–1926.

Coleman, D.S., Glazner, A.F., Miller, J.S., Bradford, K.J., Frost, T.P., Joye, J.L., and Bachl, C.A., 1995, Exposure of a Late Cretaceous layered mafic-felsic magma system in the central Sierra Nevada batholith, California: Contributions to Mineralogy and Petrology, v. 120, p. 129–136.

Didier, J., and Barbarin, B., 1991, Review of the main hypotheses proposed for the genesis and evolution of mafic microgranular enclaves, *in* Didier, J., and Barbarin, B., eds., Enclaves and granite petrology: Amsterdam, Elsevier, 625 p.

Dorais, M., Whitney, J.A., and Roden, M.F., 1990, Origin of mafic enclaves in the Dinkey Creek pluton, central Sierra Nevada batholith, California: Journal of Petrology, v. 31, p. 853–881.

Fleck, R.J., Kistler, R.W., and Wooden, J.L., 1996, Geochronological complexities related to multiple emplacement history of the Tuolumne intrusive suite, Yosemite National Park, California: Geological Society of America Abstracts with Programs, v. 28, no. 5, p. 65–66.

Frost, T.P., and Mahood, G.A., 1987, Field, chemical, and physical constraints on mafic-felsic magma interaction in the Lamarck Granodiorite, Sierra Nevada, California: Geological Society of America Bulletin, v. 99, p. 272–291.

Fullagar, P.D., Goldberg, S.A., and Butler, J.R., 1997, Nd and Sr isotopic characterization of crystalline rocks from the southern Appalachian Piedmont and Blue Ridge, North and South Carolina, *in* Sinha, A.K., Whalen, J.B., and Hogan, J.P., eds., The nature of magmatism in the Appalachian orogen: Geological Society of America Memoir 191, p. 165–179.

Furman, T., and Spera, F.J., 1985, Co-mingling of acid and basic magma with implications for the origin of mafic I-type xenoliths: Field and petrochemical relations of an unusual dike complex at Eagle Lake, Sequoia National Park, California, U.S.A.: Journal of Volcanology and Geothermal Research, v. 24, p. 151–178.

Hart, S.R., 1984, A large scale isotope anomaly in the Southern Hemisphere mantle: Nature, v. 309, p. 753–757.

Hildreth, W., 1981, Gradients in silicic magma chambers: Implications for lithospheric magmatism: Journal of Geophysical Research, v. 86, p. 10 153–10 192.

Hirt, W.H., and Glazner, A.F., 1995, Sr and Nd isotopic compositions of granitoids from the Mount Whitney intrusive suite, southern Sierra Nevada, California: EOS (Transactions of the American Geophysical Union), v. 76, p. F657.

Huber, N.K., Bateman, P.C., and Wahrhaftig, C., 1989, Geologic map of Yosemite National Park and vicinity, California: U.S. Geological Survey Miscellaneous Investigations Series Map I-1874, 1 sheet, scale 1:125 000.

Kistler, R.W., Chappell, B.W., Peck, D.L., and Bateman, P.C., 1986, Isotopic variation in the Tuolumne Intrusive Suite, central Sierra Nevada, California: Contributions to Mineralogy and Petrology, v. 94, p. 205–220.

Klein, E.M., and Karsten, J.L., 1995, Ocean-ridge basalts with convergent-margin geochemical affinities from the Chile Ridge: Nature, v. 374, p. 52–57.

Ludwig, K.R., 1989, Pb-Dat: A computer program for processing raw Pb-U-Th isotope data: U.S. Geological Survey Open-File Report 88–557, 37 p.

Ludwig, K.R., 1990, Isoplot: A plotting and regression program for radiogenic isotopic data: U.S. Geological Survey Open-File Report 90-91, 39 p.

Ludwig, K.R., 1998, On the treatment of concordant uranium-lead ages: Geochimica et Cosmochimica Acta, v. 62, p. 665–676.

Menzies, M.A., 1989, Cratonic, circumcratonic and oceanic mantle domains beneath the western United States: Journal of Geophysical Research, v. 94, p. 7899–7915.

Miller, J.S., Glazner, A.F., Walker, J.D., and Martin, M.W., 1995, Geochronologic and isotopic evidence for Triassic–Jurassic emplacement of the eugeoclinal allochthon in the Mojave Desert region, California: Geological Society of America Bulletin, v. 107, p. 1441–1457.

Ormerod, D.S., Hawkesworth, C.J., Rogers, N.W., Leeman, W.P., and Menzies, M.A., 1988, Tectonic and magmatic transitions in the Western Great Basin, USA: Nature, v. 333, p. 349–353.

Ratajeski, K., 1999, Field, geochemical, and experimental study of mafic to felsic plutonic rocks associated with the intrusive suite of Yosemite Valley, California [Ph.D. dissertation]: Chapel Hill, University of North Carolina, 196 p.

Ratajeski, K., and Sisson, T.W., 1999, Loss of iron to gold capsules in rock-melting experiments: American Mineralogist, v. 84, p. 1521–1527.

Reid, J.B., Jr., Evans, O.C., and Fates, D.G., 1983, Magma mixing in granitic rocks of the central Sierra Nevada, California: Earth and Planetary Science Letters, v. 66, p. 243–261.

Sisson, T.W., Grove, T.L., and Coleman, D.S., 1996, Hornblende gabbro sill complex at Onion Valley, California, and a mixing origin for the Sierra Nevada batholith: Contributions to Mineralogy and Petrology, v. 126, p. 81–108.

Stern, T.W., Bateman, P.C., Morgan, B.A., Newell, M.F., and Peck, D.L., 1981, Isotopic U-Pb ages of zircon from the granitoids of the central Sierra Nevada: U.S. Geological Survey Professional Paper 1185, 17 p.

Tatsumoto, M., Knight, R.J., and Allègre, C.J., 1973, Time differences in the formation of meteorites as determined from the ratio of lead–207 to lead–206: Science, v. 180, p. 1279–1283.

Tobisch, O.T., McNulty, B.A., and Vernon, R.H., 1997, Microgranitoid enclave swarms in granitic plutons, central Sierra Nevada, California: Lithos, v. 40, p. 321–339.

Truschel, J.T., 1996, Petrogenesis of the Fine Gold Intrusive Suite, Sierra Nevada batholith [M.S. thesis]: Northridge, California State University, 137 p.

Van Kooten, G.K., 1981, Pb and Sr systematics of ultrapotassic and basaltic rocks from the central Sierra Nevada, California: Contributions to Mineralogy and Petrology, v. 76, p. 378–385.

Wiebe, R.A., 1993, The Pleasant Bay layered gabbro-diorite, coastal Maine: Ponding and crystallization of basaltic injections into a silicic magma chamber: Journal of Petrology, v. 34, p. 461–489.

Wiebe, R.A., 1996, Mafic-silicic layered intrusions: The role of basaltic injections on magmatic processes and the evolution of silicic magma chambers: Transactions of the Royal Society of Edinburgh: Earth Sciences, v. 87, p. 233–242.

Zartman, R.E., 1974, Lead isotopic provinces in the Cordillera of the western United States and their geologic significance: Economic Geology, v. 69, p. 792–805.

Manuscript Received by the Society December 20, 1999
Revised Manuscript Received December 19, 2000
Manuscript Accepted May 1, 2001

Printed in the USA